

MICHIGAN STATE LIBRARIES
3 1293 01766 5062

This is to certify that the

dissertation entitled

ACCURACY OF SOIL PROPERTY MAPS FOR SITE-SPECIFIC MANAGEMENT

presented by

Thomas G. Mueller

has been accepted towards fulfillment of the requirements for

Ph.D. degree in Soil Management

Date December 16, 1998

MSU is an Affirmative Action/Equal Opportunity Institution

LIBRARY Michigan State University

PLACE IN RETURN BOX to remove this checkout from your record. TO AVOID FINES return on or before date due.

DATE DUE	DATE DUE	DATE DUE

1/98 c/CIRC/DateDue.p65-p.14

ACCURACY OF SOIL PROPERTY MAPS FOR SITE-SPECIFIC MANAGEMENT

By

Thomas G. Mueller

A DISSERTATION

Submitted to
Michigan State University
in partial fulfillment of the requirements
for the degree of

DOCTOR OF PHILOSOPHY

Department of Crop and Soil Science

ABSTRACT

ACCURACY OF SOIL PROPERTY MAPS FOR SITE-SPECIFIC MANAGEMENT

By

Thomas G. Mueller

The accuracy of soil property maps for site-specific management may be inadequate at sampling intensities recommended by commercial agriculture. Since the success of site-specific fertilizer applications depends on the quality of soil property maps, it is critical for Michigan farmers who are adopting these practices to have an understanding of the accuracy associated with different soil sampling strategies, soil sampling intensities, and interpolation techniques. This thesis evaluates how grid sampling and interpolation schemes affected map accuracy based on measures of map error. The second objective was to evaluate how different interpolation techniques that incorporate terrain attributes affects the spatial predictions of soil properties and whether relative performance of these techniques is affected by the scale of soil sampling. In addition to the soil samples used for spatial interpolation, samples were collected to assess the quality of the predictions. Grid point sampling at the industry standard intensity (100 m regular grid), grid cell sampling (100 m grid cells) and directed sampling based on soil type were not adequate to produce accurate nutrient condition maps for this field even though most of the variables were spatially structured. Prediction efficiencies were 0.5 to 10.5 % greater for inverse distance weighted interpolation than for kriging using a distance exponent of 1.5 at the 30-m grid sampling intensity. At high

sampling densities (30 m regular grid), interpolation methods that utilized terrain attributes had similar prediction errors to interpolation methods that did not utilize terrain attributes. At a lower sampling intensity (61 m regular grid), methods that utilized terrain attributes, especially multiple regression, were more accurate than methods that did not. At the 61 m grid, the RMSE for multiple regression was lower (3.3 g kg⁻¹) than the RMSE for ordinary kriging (4.1 g kg⁻¹). A 100 m grid was not of sufficient intensity to be used to create accurate maps of soil properties for site-specific nutrient management, enhancing spatial estimates with terrain attributes can reduced the number of samples required to create an accurate map. It was not necessary to use complex, time consuming geostatistical techniques to use terrain attributes because multiple regression was sufficient.

Copyright by Thomas G. Mueller 1998 This dissertation is dedicated

to my wife, Angela, for her love and perseverance;

to our parents, Philip, Camille, Peter, and Gabriela, for their support and encouragement,

and to our children, Daniel and Christina, for the joy they have given us,

ACKNOWLEDGMENTS

I would like to thank Dr. Francis J. Pierce believing in me and for his friendship, guidance, encouragement, and financial support. I would also like to express my gratitude to Dr. Darryl Warncke for serving as the co-chair of my graduate committee and for his helpful advice. I am very grateful to both Dr. G. Philip Robertson and Dr. Irvin E. Widders for their advice and for serving on my committee. Again, I would like to thank my entire committee for their precious time.

A special thanks goes to the farmers, John Anibal and Patrick Feldpausch, for there generosity. Also thanks to Jim Walseth at Springhill Engineering for mapping elevation at one of the research locations. Also thanks to Steve Law at the NRCS office in Clinton County for his help soil sampling.

I am grateful to Dr. Oliver Schabenberger for many hours of consultation. I appreciate the invaluable advice of Dr. Pierre Goovaerts from the University of Michigan. I am especially grateful to Dr. Jose E. Cora for his friendship and collaboration. I am also grateful to for the technical assistance of Brian Long. I also would like to thank Cal Bricker for his advice and friendship. Thanks to Brian Long, Cal Bricker, and Gary Zehr for their help in the field near Kalamazoo.

I appreciate the friendship and technical assistance of Brian Baer, Sven Bohm, Dr. Dave Harris, Dr. Samira Daroub, Brian Graff, and Elaine Parker. Thanks also goes to Dan Brown for teaching two very useful classes in GIS and for being so helpful. A special thanks goes to Demetrios Gatziolis for help with GIS and his friendship. I also appreciate the help of Jon Dahl and Vickie Smith from the Michigan State University soil testing laboratory for always being so helpful with research and teaching soil samples.

Thanks for all of the hard work to the students I have supervised: Curtis Beard,
Bill Bower, Frank Boyd, Raulie Casteel, Jolene Friedland, Jeanette Makries, and Edwin
Toledo. I appreciate their friendship and their hard work.

Thanks to Dr. Daniel Rasse, Dr. Joseph Masabni, Mohamed Elwade, James Sallee, and Djail Santos, Laurent Gilet, Carlos Paglis and Dr. Helvecio De-Polli, and Dr. Tom Willson, and Jeff Smeenk for their friendship.

TABLE OF CONTENTS

LIST OF TABLES	ix
LIST OF FIGURES	x
INTRODUCTION	1
Prediction Errors and Efficiencies	
Spatial Interpolation	
•	٠
CHAPTER 1 ASSESSING MAP ACCURACY FOR SITE-SPECIFIC	_
FERTILITY MANAGEMENT	
INTRODUCTION	
MATERIALS AND METHODS	
Site description	
Soil Sampling Design and Laboratory Analysis	
Data Analysis	
Phase I: FULL data set	
Phase II: Accuracy of SSFM sampling and interpolation	
RESULTS AND DISCUSSION:	
Phase I. FULL Data Set.	
Phase II: Accuracy of SSFM sampling and interpolation	
Grid Sampling	
CELL and directed sampling	
CONCLUSIONS	38
CHAPTER 2 COMPARISON OF TECHNIQUES TO OPTIMIZE	
SPATIAL ESTIMATES OF SOIL PROPERTIES USING	
TERRAIN ATTRIBUTES	40
INTRODUCTION	
MATERIALS AND METHODS	
Site description	
Soil Sampling Design and Laboratory Analysis	
DEM Creation and Terrain Analysis	
Data Analysis	
RESULTS AND DISCUSSION	
Nature of the Data	
Evaluation of Interpolation Methods	
CONCLUSIONS	
SUMMARY AND RECOMENDATIONS	
RIBLIOGRAPHY	

LIST OF TABLES

Table 1.1	Map symbols, soil series or complex name, NRCS soil taxonomic	
	description (Pregitzer, 1978), and area occupied in the field	.10
Table 1.2.	Data set descriptions	.13
Table 1.3.	Summary statistics for the FULL data set.	.16
Table 1.4.	Directional and omnidirectional semivariogram model parameters for the FULL data set	.22
Table 2.1.	Applications of regression, kriging with an external drift, and cokriging for enhancing spatial estimates of soil properties using	.41
Table 2.2.	Directional (G ₃₀) and omnidirectional (G ₃₀ and G ₆₁) semivariogram model parameters for carbon to be used for ordinary kriging	.55
Table 2.3.	Correlations between total carbon and terrain attributes and explained variability (G ₃₀ data set)	.56
Table 2.4.	Linear model of coregionalization (G ₃₀) used for cokriging	.57
Table 2.5.	Semivariogram model parameters fo the direction of maximum spatial continuity (N 90 E) for kriging with a trend model and	6.0
	kriging with an external drift	.57

LIST OF FIGURES

_	Modeled empirical semivariogram
Figure 1.3.	Normal probability (Q-Q) plots for variables and log transformations with 95% confidence intervals
Figure 1.4.	Directional variogram contour maps for the FULL data set20
Figure 1.5.	Directional and omnidirectional semivariograms for the original
	and transformed FULL data sets21
Figure 1.6.	Contour maps of kriged soil variables and fertilizer
	recommendations using the FULL data sets overlain by the soil
7	type boundaries
Figure 1.7.	Omnidirectional experimental and modeled (exponential)
T: 10	semivariogram for the FULL, G _{comb} , G ₃₀ , G ₆₁ , and G ₁₀₀ data sets 27
Figure 1.8.	The RMSE for several estimation approaches: IDW interpolation
	for distance exponents ranging from 0.1 to 5.0 in 0.1 increments
	(line plots on the left), kriging, whole field, and grid cell
F: 1 O	sampling; and zone sampling
Figure 1.9.	The relationship between the optimal distance exponent and the
E: 1 10	CV
rigure 1.10	Predicted vs. measured for kriging with the G _{comb} , G ₃₀ , and G ₁₀₀ data sets
Eigung 1 11	
riguie 1.11	The relationship between prediction efficiency for kriging the G30 data set, the range of spatial correlation of the FULL data
	set, and the RSV of the FULL data set
Figure 1 12	The relationship between prediction efficiency for the kriged G_{30}
riguie 1.12	data set and the range of spatial correlation for the FULL data set
	for variables with RSV values greater than 70%34
Figure 1 13	Prediction efficiency for kriging versus the prediction efficiency
riguic 1.15	for IDW
Figure 1.14	. Average semivariograms (large solid circles) and
B	semivariograms for individual pairs (hallow circles) for P using
	the G _{comb} data set.
Figure 2.1	Study location: (a) areal photograph and (b) soil and kinematic
1 1guio 2.1.	GPS measurement locations overlain by soil type boundaries46
Figure 2.2	Surface maps (a) of elevation and (b) slope and a contour map
I Iguit 2.2.	(c) of elevation overlain with arrows indicating aspect
Figure 2.3	Normal probability (Q-Q) plots for variables and log
5	transformation with 95% confidence intervals
Figure 2.4.	Semivariogram surfaces for total carbon (G_{30}) and elevation $(n =$
0	1000)

Figure 2.5. Total carbon (g kg ⁻¹) contour r	nap created with ordinary kriging
using the G ₃₀ data set overlain	with elevation contours (lines)55
Figure 2.6. Prediction efficiencies and RM	ISE's59
Figure 2.7. Predicted versus measured val	ues for several prediction methods
at two scales of measurement.	60
Figure 2.8. The relationship between pred	iction efficiency and sample point
density for multiple regression	interpolation62
Figure 2.9. Predicted total carbon (g kg ⁻¹)	using kriging with an external drift
(G ₃₀) and multiple regression (G_{30} and G_{61})64

INTRODUCTION

Precision agriculture is about managing soil and crop variability in space and time in order to improve crop performance and environmental quality (Pierce and Nowak, 1999). Soil chemical and physical properties and crop yield are spatially quite variable. While some attributes are stable over time (e.g. total carbon, texture), others exhibit a great deal of temporal variability (e.g. soil N, soil water content water, grain yield, and pest infestation). The area of precision agriculture related to nutrient management is often referred to as site-specific fertility management (SSFM). In this dissertation, I am specifically concerned with the SSFM of soil nutrients that that are spatially variable but relatively temporally stable, specifically, total carbon, pH, P, K, Ca, and Mg.

Several conditions are essential for successful SSFM, the most basic of which is that variation in soil properties is adequately known (Pierce and Nowak, 1999 and Sawyer, 1994). Some of the studies that have tested the validity of this premise have shown that it is not always valid (Wollenhaupt et al, 1994; Gotway et al., 1996). Some SSFM agronomic and economic studies that have had mixed or negative results (Snyder et al., 1997; Wibawa et al., 1993; Wollenhaupt and Bucholz, 1993) might be explained by poor prediction accuracy of soil properties. Fortunately, there are good methods for measuring prediction and map accuracy.

The kriging variance can not be used to estimate the map accuracy because it is independent of the data values (Deutsch and Journel, 1998) and only dependent on the covariance model and the data configuration (Goovaerts, 1997). Cross-validation is a technique where sample data points are sequentially dropped from the prediction data set, estimated from the neighboring point, and then replaced (Deutsch and Journel, 1998).

The measured values are subtracted from the predicted values to calculate the residuals which can be used to assess the accuracy of the predictions. For a regular gridded data set, cross-validation tends to over estimate prediction errors. A better approach would be to jack-knifing with an independent validation data set. This approach was used in this dissertation. The calculation of these errors is discussed in the first section of this introduction.

The first objective of this dissertation was to evaluate how grid sampling and interpolation schemes affected map accuracy and prediction efficiency. The next objective was to evaluate different analytical techniques that using terrain attributes affect the spatial prediction of soil properties and whether relative performance of these techniques was affected by the scale of soil sampling. This dissertation requires some understanding of geostatistics, ordinary kriging, and inverse distance interpolation. The theory is presented in the second section of this introduction.

Prediction Errors and Efficiencies

In this study, measures of map error included MSE, RMSE (root mean squared error), and bias. Let v_i denote the difference between predicted value and observed value at location s_i , $i=1, ..., n_v$, where n_v is the number of values in the validation data set. A map correct on average should have $E[v_i] = 0$. The bias of the map is estimated as

$$Bias = \frac{1}{n_v} \sum_{i=1}^{n_v} v_i$$

and the MSE of the map as

MSE = Bias² +
$$\frac{1}{n_{v} - 1} \sum_{i=1}^{n_{v}} (v_{i} - v)^{2}$$

= $\frac{1}{n_{v} - 1} \sum_{i=1}^{n_{v}} v_{i}^{2}$

The RMSE is the square root of the MSE, RMSE= \sqrt{MS} . The mean square error combines accuracy (bias²) with precision, the variance of the residuals. Prediction efficiency referred to as goodness by Gotway et al. (1996) is calculated as

Prediction efficiency =
$$100\% * (MSE_{A30} - MSE_{prediction})(MSE_{A30})^{-1}$$
. [1]

Positive prediction efficiencies can be interpreted as the percent reduction in MSE as compared with the field average approach (A₃₀). A prediction efficiency of 15% for kriging can be interpreted as "compared to the field average approach, kriging reduced the MSE by 15%." The optimal distance exponent for IDW interpolation was determined as the one yielding the lowest RMSE.

Spatial Interpolation

A spatial estimator at an unobserved location s of an attribute Z is defined as a weighted average of the observed values of the attribute at spatial locations s_i . The weights $w_{S(i)}$ may be restricted to non-zero values in some neighborhood $N_{(s)}$ of the target location s. If n(s) is the number of observed values in the neighborhood, the predicted value is calculated as

$$\hat{Z}(s) = \sum_{i=1}^{n(s)} w_{S_i} Z(s_i)$$

The essential difference between kriging and IDW estimation lies in the determination of the weights. The weights w for IDW are based on the distance between the point to be estimated and each of the n sample data points $d(s_{\omega}s)$ within the search neighborhood N(s).

$$w_{\alpha} = [d(s_{\alpha}, s)]^{e} \sum_{\alpha=1}^{n(s)} [d(s_{\alpha}, s)]^{-e}$$

where e is the user defined distance exponent (Gotway, 1996). Smoothness of interpolated values decreases with the magnitude of the exponent. The kriging weights are calculated by solving the kriging system presented here in an expanded matrix form

$$\begin{bmatrix} w_1 \\ \vdots \\ w_n \\ \lambda \end{bmatrix} = \begin{bmatrix} Cov_{11} & & & Cov_{1n} & 1 \\ \vdots & & & \vdots \\ Cov_{n1} & & & Cov_{nn} & 1 \\ 1 & & & 1 & 0 \end{bmatrix}^{-1} \begin{bmatrix} Cov_{1s} \\ \vdots \\ Cov_{ns} \\ 1 \end{bmatrix}$$

where λ is a Lagrange parameter needed to satisfy certain constraints. Cov₁₁ through Cov_{nn} are the covariances among the sample data points, and C_{1s} to C_{ns} are the covariances between each sample data point and the unobserved location s (Goovaerts, 1997). For details of constrained minimization through Lagrange multipliers in this context see Isaaks and Srivastava (1989). Under weak stationarity conditions (Cressie, 1993) the covariances between two data points depends not on their actual coordinate, but

matters. Since the kriging weights are functions of the covariances which in turn depend on spatial separation of data points, kriging weights are distance related weights too. The metric in which distances are assessed is not, however, Euclidean distance alone, but depends on the degree of spatial dependencies. Under second order stationarity, the covariance model are related to semivariogram models through the relationship $Cov_{ij} = C(O) - \gamma(h_{ij})$; where C(O) is the variance and h_{ij} is the Euclidean distance between locations s_i and s_j the distance between sample locations. The semivariogram models are fit to empirical semivariograms $\lambda(h)$ which is the average sample variance of points separated by distance h but computationally defined as $\frac{1}{2}$ of the average squared difference of points separated by distance h,

$$\lambda(h) = \frac{1}{[2n(h)]} \sum_{i=1}^{n(h)} [S_{(\alpha i)} - S_{(\alpha i+h)}]^{2}$$

where n(h) is the number of pairs at lag distance h or in some neighborhood of h. Figure 1.1 illustrates an isotropic semivariogram modeled with an exponential function. The plateau the variogram reaches is called the sill. The discontinuity at the origin is referred to as the *nugget variance* and is attributable to the additive effects of a white noise process and measurement error (Cressie, 1993). The *sill* less the nugget variance is referred to as the *structural variance*. The separation distance (lag) at which the variogram reaches the plateau (spherical models) or 95% of the sill (exponential and Gaussian models) is called the *range* or *range of spatial correlation*.

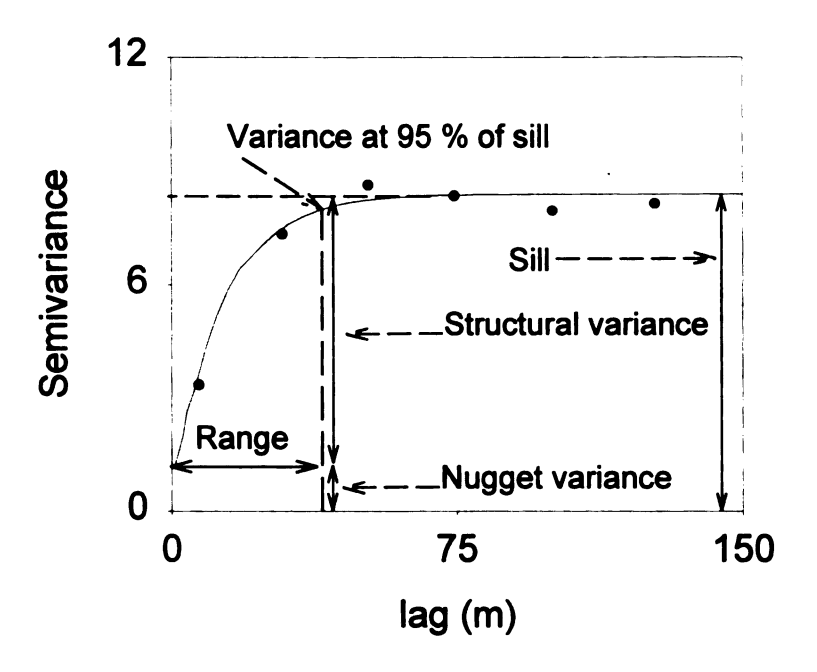


Figure 1.1. Modeled empirical semivariogram.

Relative structural variability (RSV) was used as a normalized measure of spatial dependence (Robertson et al., 1993; 1997) and is defined as

$$RSV = \frac{\text{structural variance}}{\text{sill}} = 1 - RNE$$
 [2]

and is related to what is commonly referred to as the relative nugget effect (RNE).

CHAPTER 1

Assessing Map Accuracy for Site-Specific Fertility Management

INTRODUCTION

Several conditions are essential for successful site-specific fertility management (SSFM). The most basic condition is that variation in soil properties is adequately known (Pierce and Nowak, 1999 and Sawyer, 1994). Soil property predictions across landscapes are affected by soil sampling, laboratory analysis, prediction, and cartographic errors. Poor map quality may explain why results of some SSFM agronomic and economic studies have had mixed or negative results (Snyder et al., 1997; Wibawa et al., 1993; Wollenhaupt and Bucholz, 1993). Some have suggested alternatives to grid sampling, including directed sampling (Pocknee et al., 1996). In general, condition and management maps are rarely examined for quality, which is unfortunate because methods exist to assess map accuracy.

Measures of accuracy and goodness have been used in SSFM research to assess quality of maps and soil properties predictions, mostly by studying the impact of grid sampling intensity (Wollenhaupt et al., 1994; Franzen and Peck, 1995; Gotway et al., 1996, Mohamed et al., 1996) and interpolation techniques (Wollenhaupt et al., 1994; Gotway et al., 1996, Mohamed et al., 1996) on map or prediction error. Wollenhaupt et al. (1994) and Mohamed et al. (1996) considered map accuracy to be the percentage of areal overlap of mapping categories between maps in question and maps considered representative of the true spatial distribution of a soil property in space. These truth maps

were arbitrarily defined to be contour maps created either with Delaunay triangulation of soil properties sampled at a 32-m grid (Wollenhaupt et al., 1994) or with the kriging of soil properties sampled on a 20 x 40-m grid (Mohamed et al., 1996).

The correlation between predicted and observed data sets has been used as a measure of prediction accuracy (Franzen and Peck, 1995; Goovaerts, 1997). A correlation approach alone is problematic. While predicted and observed data sets may be highly correlated, they may deviate greatly from a 1:1 relationship and therefore be of low predictive value in a mapping context. Franzen and Peck (1995) assessed map error by assigning both measured values and their associated predictions to classes and then determining the percentage of measured values that were assigned to the same class as their predictions.

Gotway et al. (1996) used mean square error (MSE) as a measure of prediction accuracy calculated using independent validation data sets. Map goodness was calculated by comparing the MSE for interpolation to the MSE for the field average approach. To a large extent, the appropriate grid spacing depends on the spatial structure of soil properties (Sadler et al., 1998) and the range of spatial correlation (Mohamed et al., 1996). Furthermore, the appropriate interpolation method may depend on specific coefficients of the interpolation procedure used. For example, the optimal distance exponent for the inverse distance weighted (IDW) interpolation procedure may depend upon the coefficient of variation (CV; Gotway et al., 1996).

While grid sampling and interpolation approaches have limitations, a shift from grid sampling to directed sampling schemes or grid cell based approaches may not improve map accuracy. Directed sampling is a technique wherein samples are collected

and composited from specified areas within a field. Pocknee et al. (1996) suggest that the areas be delineated based on established differences within a field. Differentiating criteria might include soil map delineations (Bell et al., 1995, Moore et al., 1993, Windawa et al. 1993), management history, yield potential maps, aerial imagery (McCann et al., 1996; Pocknee et al., 1996), or electromagnetic induction (Jaynes, 1996). Directed sampling techniques require prior knowledge about the factors that regulate crop yield and nutrient availability. In general, map or prediction errors associated with directed sampling schemes have not been reported. Instead of sampling on grid points, composite samples can be taken from the area between grid points, a practice that is referred to as grid cell sampling. Grid cell sampling schemes have not found extensive use in SSFM. This may be related to earlier reports that grid point sampling more accurately described soil properties than did grid cell sampling, such as that reported by Wollenhaupt et al. (1994) for two fields in central Wisconsin.

The purpose of this study was to evaluate how grid sampling and interpolation schemes affect map accuracy based on measures of bias, precision, and prediction efficiency, or what Gotway et al. (1996) termed goodness. For this study, a field was subjected to several soil sampling strategies including grid point sampling at several grid spacings, grid cell sampling, and directed sampling based on soil type. Soil fertility and fertilizer recommendation data were interpolated using kriging and a range of IDW coefficients for the various sampling schemes. Each resulting prediction map was tested against a random validation set to evaluate map accuracy.

MATERIALS AND METHODS

Site description

This study was conducted within a 20.4-ha field (42° 57′ 54″ N, 84° 43′ 38 W) in Clinton County, Michigan, 6-km south of Fowler. The field has been in a corn (Zea mays L.)-soybean (Glycine max L. (Merr.)) rotation for 22 years and the southeastern portion of the field has been sub-irrigated since 1988. The field was selected because it contained multiple soil map units and exhibits a range of terrain features, both of which would be conducive to SSFM. Pregitzer (1978) described and mapped the soils in Clinton County, MI at a scale of 1:15,840. The great group taxonomic classifications of the soils in this field were either Ochraqualfs (Capac and Metamora) or Hapludalfs (Morley and Wasepi; Table 1.1). The soils were somewhat poorly drained except for the Morley, which was moderately well drained. All of the soils formed in glacial till except for the Wasepi, which formed in loamy glaciofluvial deposits.

Table 1.1 Map symbols, soil series or complex name, NRCS soil taxonomic description (Pregitzer, 1978), and area occupied in the field

Symbol	Name and slope	Taxonomic Family and Subgroup	Area (ha)
MoB	Morley loam	Fine, illitic, mesic	1.3
	(2 to 6 % slope)	Typic Hapludalfs	
CaA	Capac loam	Fine-loamy, mixed, mesic	7.2
	(0 to 4 % slope)	Aeric Ochraqualfs	
MeA	Metamora-Capac sandy	Fine-loamy, mixed, mesic	8.9
	loams (0 to 4 % slope)	Udollic and Aeric Ochraqualfs	
WbA	Wasepi sandy loam (0 to 3 % slope)	Coarse-loamy, mixed, nonacidic, mesic Aquollic Hapludalfs	3.0

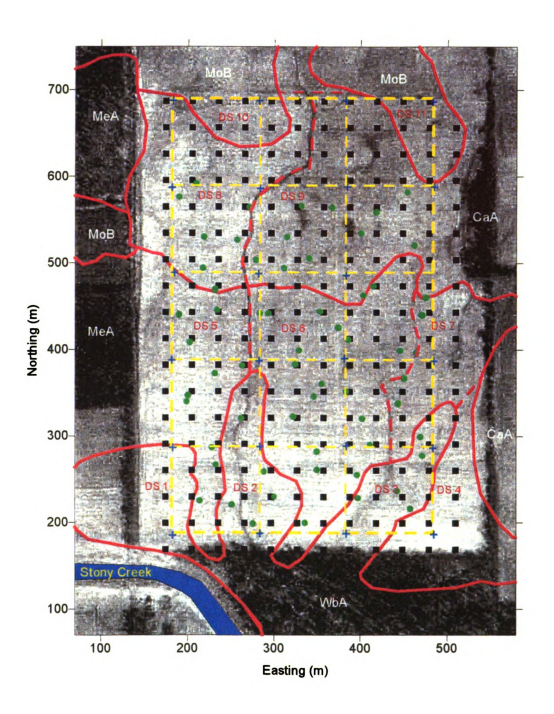


Figure 1.2. A digital orthophotograph overlain by the 30 m (black square), the 100 m (blue cross), the random validation data set (green circle) and NRCS soil types (CaA = Capac loam with 0 to 4 % slope; MeA = Metamora-Capac sandy loam with 0 to 4% slope; MoB = Morley Loam with 2 to 6% slope; and WbA = Wasepi sandy loam with 2 to 6% slope).

† red solid and dashed lines indicate boundaries of directed sampling zones (DS 1-11) and dashed yellow lines indicate the boundaries of the CELL based sampling.

Soil Sampling Design and Laboratory Analysis

Soil samples were obtained from the field using four sampling designs: a 30.5-m regular grid, a 100-m grid cell, a 200-m unaligned grid, and random sample design. These samples were used as data sets or to calculate data sets as described in Table 1.2. The sample point locations were flagged using a DGPS system with a base station for onthe-go differential correction. At each grid and randomly distributed point, 5 subsamples (1 at the grid point and 4 within a 1.5-m radius) were obtained to a depth of 20cm using a 2.5-cm diameter core and composited. The grid cell samples were taken by compositing 9 individual cores of the same diameter and depth taken at regular intervals within each 100-m grid cell (Figure 1.2). Soils were dried under forced air at 35° C for 3 days and ground to pass a 2-mm sieve. Standard soil analyses were conducted by the Michigan State University Soil and Plant Nutrient Laboratory using the recommended chemical soil test procedures for the North Central Region (Brown, 1998). Analyses included pH (1:1 soil water mixture), BpH (SMP buffer), P (Bray P-1 extractable) K, Ca, and Mg (1M/L NH₄OAc extractable). Cation exchange capacity (CEC) was calculated by summation and lime (L_{rec}), P (P_{rec}), and K (K_{rec}) fertilizer recommendations were calculated using the tri-state fertilizer recommendations (Vitosh et al., 1995) for corn with a uniform yield goal of 11.3 Mg ha⁻¹ (180 bu acre⁻¹).

Table 1.2. Data set descriptions

Name	N	Description
		Prediction Data Sets
G ₃₀	215	Soil samples taken on a 30-m regular grid.
G_{100}	24	Soil samples taken on a 100-m regular grid.
CELL	15	Soil samples taken in 100-m grid cells
G_{comb}	239	Created by combining G ₃₀ and G ₁₀₀ grid data sets.
G_{61} -a G_{61} -b G_{61} -c G_{61} -d	54 54 54 53	Created by separating the 30-m grid data set into four separate 61-m grids. Each grid was analyzed separately, but the results are given as the average results from the four grids.
DIR	11	Created by overlaying the soil map units onto the 30-m grid and determining the mean fertility value for each management unit.
A ₃₀	1	Field average value for the entire field calculated from the means of the 30-m grid.
A ₁₀₀	1	Field average value for the entire field calculated from the means of the 100-m grid.
		Validation Data Set
VAL	62	Independent validation created by combining a 200-m unaligned grid with additional random samples.
	Dat	ta set for geostatistical analyses
FULL	301	Created by combining G ₃₀ , G ₁₀₀ , and VAL.

Data Analysis

Data analysis was performed in two phases. Phase I involved a quantitative analysis of the FULL data set, which consisted of the combination of the G_{30} , the G_{100} , and the random (VAL) data sets (Table 1.2). The purpose of Phase I was to assess the extent to which the spatial variability of soil fertility in this field lends itself to SSFM. The steps in phase I included an assessment of normality, calculation of descriptive statistics, and analysis of spatial variability. Phase II was an assessment of the accuracy of sampling designs and interpolation procedures using quantitative measures of map quality.

Phase I: FULL data set

The FULL data set consisted of the 301 sample locations corresponding to an average sampling intensity of 14.8 samples ha⁻¹ (Table 1.2). Normal probability (Q-Q) with 95 % confidence intervals (Friendly, 1991) were used to assess normality of the FULL data set. When the Q-Q normal probability plots indicated large deviations from normality, the natural log of these variables was calculated and the resultant tested for normality. If the log transformations were also non-normal, then the original variables were power transformed and again tested for normality. The power transformations were not successful in inducing normality and will not be discussed further. Finally, normal score transformations (Deutsch and Journel, 1998; Goovaerts, 1997) were used to normalize the remaining variables that could not be normalized with log or power transformations. Contour maps of variogram surfaces were created for each original variable to determine the direction of the anisotropic axes if anisotropy existed

(Goovaerts, 1997; Isaaks and Srivastava, 1989). For directional (anisotropic) semivariograms, an angular tolerance of ± 40° was used because it allowed the variograms to be well defined while still preserving their essential features (Isaaks and Srivastava, 1989). Nested semivariogram models (combinations of spherical, exponential, and/or Gaussian models) were chosen based on their fit to the empirical variograms, if warranted. Using the modeled semivariograms, GSLIB (Deutsch and Journel, 1998) was used to create kriged 4 by 4-m grids at search radii equal to the distances to which the semivariograms were modeled. Contour maps for each kriged grid were created with Surfer® (Golden Software, Golden, CO).

Phase II: Accuracy of SSFM sampling and interpolation

Phase II was concerned with how different sampling schemes and estimation procedures affected map accuracy. For the FULL, G₃₀, G_{61a-d}, G₁₀₀, and G_{comb} grid data sets, empirical semivariograms were calculated using Variowin (Pannatier, 1996) and an omnidirectional exponential model was fit to the empirical semivariograms. Surfer was used to interpolate 4 x 4 m grids by kriging each data set with the modeled semivariogram and using IDW for distance exponents from 0.1 to 5.0 in 0.1 increments. For comparison purposes, omnidirectional semivariograms based on an exponential model were also developed for the FULL data set.

To quantify the error of prediction for each attribute, sampling scheme, and interpolation method, the difference between the predicted surface and the validation points were estimated. Since the VAL points did not always coincide with the 4 x 4 m predicted grid locations, bilinear interpolation in Surfer was used to estimate the predicted value at each VAL grid location. Because only one value is assigned to each

soil management unit, each cell, and to the entire field, residuals for the DIR, CELL, A_{30} , and A_{100} predictions were calculated as the distance between the VAL points and the measured value for the area containing that point. Prediction errors and efficiencies were calculated as described in Chapter 1.

RESULTS AND DISCUSSION:

Phase I. FULL Data Set.

While the average soil tests for this field indicated that soil fertility was adequate, there was considerable range in each parameter (Table 1.3), indicating that some portion of the field may respond to SSFM. For SSFM to be applicable to this field, the variation of soil fertility must be spatially structured, of sufficient magnitude, and within the manageable range. Semivariance analysis was conducted to quantify the extent to which these conditions were met.

Table 1.3. Summary statistics for the FULL data set.

Variate	mean	Median	Min	Max	CV (%)
pH	6.1	6.0	5.2	8.0	9
P (mg kg ⁻¹)	26	25	8	86	44
K (mg kg ⁻¹)	167	165	95	291	23
Ca (mg kg ⁻¹)	1482	1450	650	3053	22
Mg (mg kg ⁻¹)	274	267	80	474	23
CEC (cmole kg ⁻¹)	13.0	13.0	7.7	20.5	17
L _{rec} (Mg ha ⁻¹)	4	5	0	13	76
Prec (kg ha ⁻¹)	63	75	0	114	42
K _{rec} (kg ha ⁻¹)	25	0	0	100	136

[†] Min = minimum, Max = maximum.

While normality is not a requirement for developing a semivariogram or kriging, the classical linear kriging predictor does not retain optimal properties if the underlying spatial process is not Gaussian (Cressie, 1993). Only Mg and CEC were normally distributed, while P, K and Ca were log-normally distributed (Figure 1.3, Table 1.3). Soil pH, L_{rec}, P_{rec}, and K_{rec} could not be transformed to normality with log or power transformations but could be through a normal score transformations (Figure 1.3). The reason L_{rec}, P_{rec}, and K_{rec} deviated so drastically from normality is because the tri-state lime and fertilizer recommendations (Vitosh et al., 1995) combine stair stepping, nested functions. Because of the nature of these calculations, however, the back transformations for the normal score transformations of L_{rec}, P_{rec}, and K_{rec} were problematic and therefore should not be used for SSFM of this field. It may be that native Mg and CEC levels were distributed normally and remained so because lime applications have been primarily calcitic and CEC has minimally been affected by management practices. In another geospatial study in Michigan, soil properties in an uncultivated landscape appeared to be distributed more normally than those in an adjacent cultivated field (Robertson et al., 1993).

Anisotropy occurs when the semivariogram depends not only on separation distance, but also on the angular relationships between data points. The presence and direction of anisotropy must be known to create anisotropic models and can easily be detected and measured using contour maps of semivariogram surfaces (Goovaerts, 1997). Only CEC and L_{rec} were considered to be isotropic (Figure 1.4). Directional or

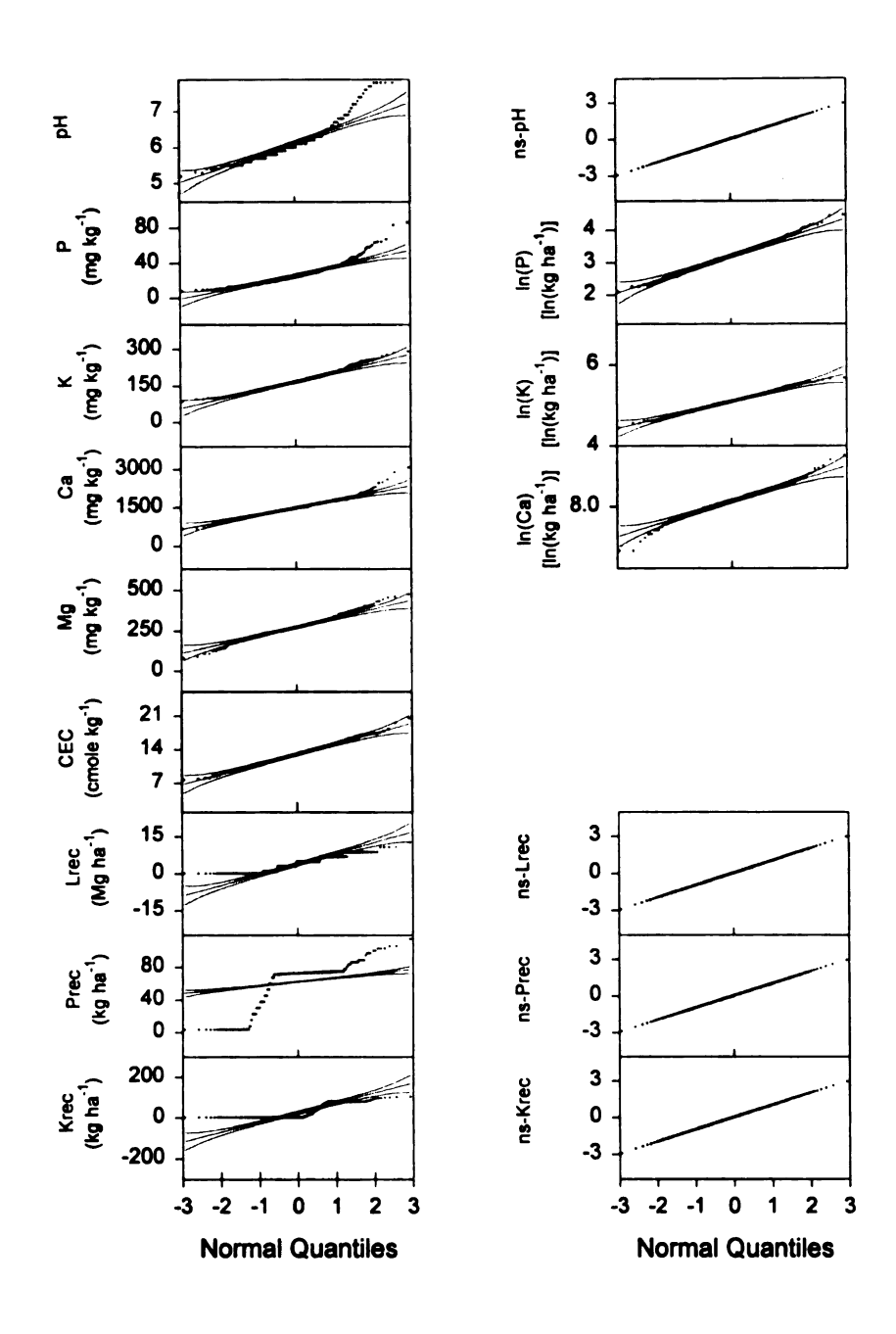


Figure 1.3. Normal probability (Q-Q) plots for variables and log transformations with 95% confidence intervals.

† ns indicates a normal score transformation; pH already log transformed

omnidirectional semivariograms were calculated and modeled for each variable and their normal transformations (Figure 1.5). The semivariogram models accounted for geometric (range changes with direction, sill does not) and zonal (sill changes with direction; range does not) anisotropy and mixtures of both (Isaaks, and Srivastava, 1989). The directional and non directional variograms were described with one, two, or three nested spherical, exponential, or Gaussian transitional structures in addition to a nugget structure (Figure 1.5 and Table 1.4). Overall, anisotropy was not severe and, removable with transformations (pH and Ca). It would not be cost effective for anisotropy to be modeled for this field on a commercial basis because the anisotropy is not strong, its modeling time and resource expensive, and the coarseness of commercially accepted SSFM would not allow the short range anisotropy to be resolved.

The kriging system of equations requires that a second order stationary model be fit to the empirical semivariograms. Second order stationarity can be inferred the semivariogram reaches a plateau as occurred for most variables (Figure 1.5). When semivariograms do not reach a plateau, intrinsic stationarity is often assumed (Pannatier, 1996). But, by limiting the search radius, a stationary model can still be applied. The semivariograms for pH in the N 54° E direction and and Ca in the N 49° E direction exhibited intrinsic stationarity in these directions. This behavior was attributable to a "hot spot" in the southwestern corner of the field where lime had been stored (Figure 1.6) rather than a gradual trend in the data. Normalizing the pH and Ca data removed the directional, intrinsic behavior. Second order and intrinsic stationarity was assumed for the FULL data set and issues of non-stationarity are irrelevant for SSFM management of this field.

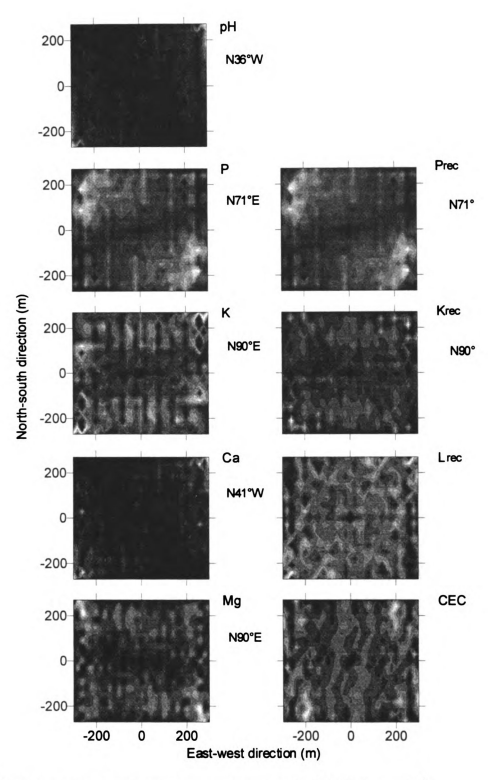


Figure 1.4. Directional variogram contour maps for the FULL data set. †

† white and black represent the minimum and maximum semivariogram, respectively of the FULL data set (not transformed).

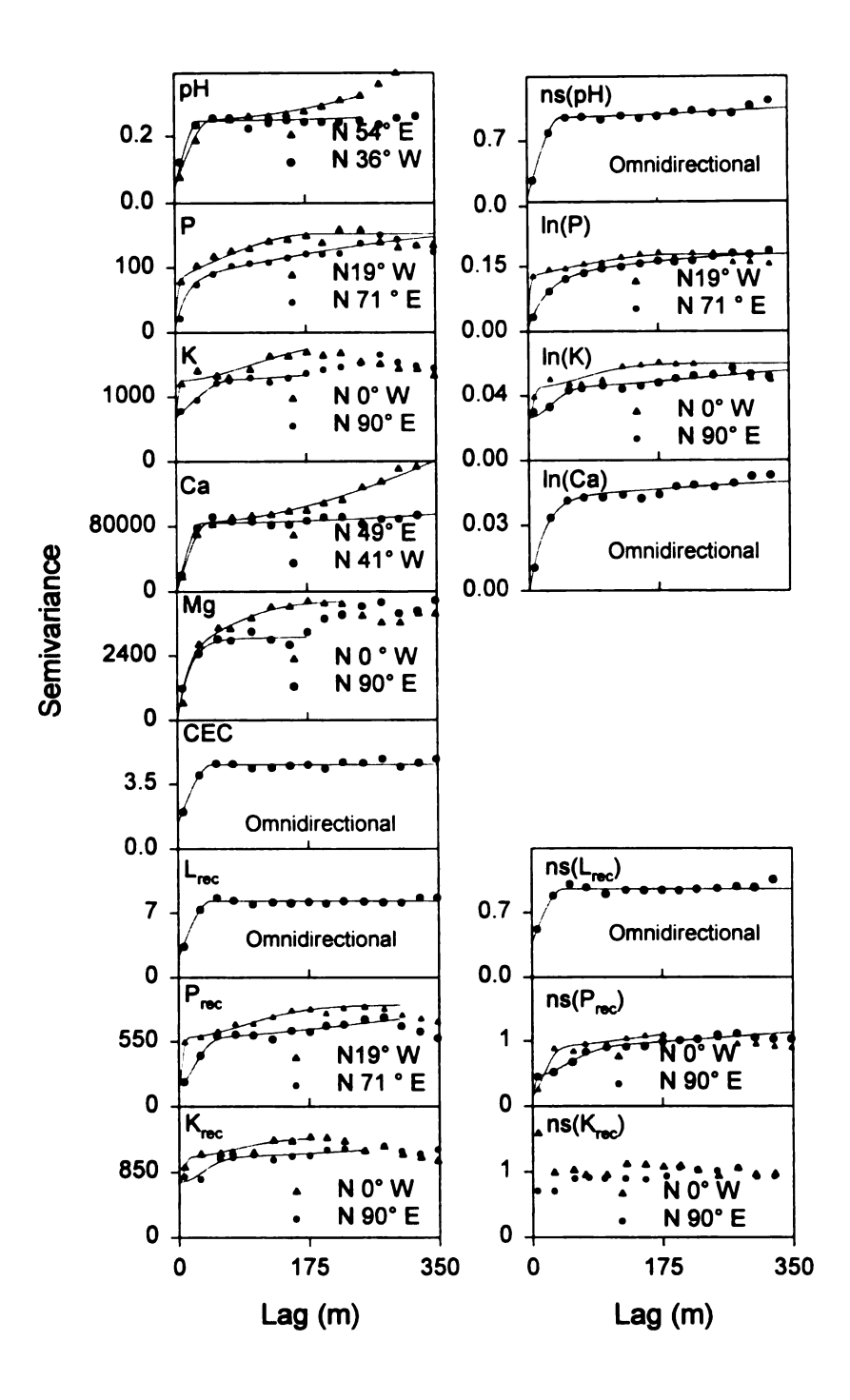


Figure 1.5. Directional and omnidirectional semivariograms for the original and transformed FULL data sets. †

† ns indicates a normal score transform.

Table 1.4. Directional and omnidirectional semivariogram model parameters for the FULL data set

		ln (P) 0.01	P 34	ns-pH 0.09	pH 0.045	Variable nugget
	S	យ	m	S	S	Model [†]
	2888	0.118	381	0.86	0.20099	sill
N 90° E	N 90° E	N 71° E N 19° W	N 71° E N 19° W	0	N 36° W N 54° E	Structure 1—direction
69	77 8	79 7	45 10	46	34 56	range
:	46	92	92	91	8 2	RSV [‡]
)	G	S	S	G	G	Model
0015	3115	0.05	347	0.15	1.6	Struct
N 90° E	N 90° E	N 71° E N 19° W	N 71° E N 19° W	0	N 36° W N 54° E	-Structure 2—sill direction
550 171	800 248	350 200	450 1 8 9	600	5500 1980	range

† S = spherical, E = exponential, G = Gaussian, O = omnidirectional, ns indicates a normal score transformation ‡ RSV, Equation 2, calculated conservatively using the sill for the first structure only.

Table 1.4 Continued.

Kngc	ns-P _{rec}	Prec	ns-L _{rec}	L_{rec}	CEC	Mg	ln(Ca)	Ca	Variable
720	0.16	197	0.38	2.268	1.41	0	0	5200	nugget
G	S	G	S	S	S	ш	ĮΠ	S	Model
326	0.3	387	0.58	6.079	3.149	15330	0.044	416000	sill
N 90° E	N 0° E	N 71° E	0	0	0	N 90° E	0	N 41° W N 49° E	Structure 1—direction
73 13	9 36	52 10	43	44	46	49 46	63	23 23	range
31	65	66	60	73	69	100	100	99	RSV [‡]
G	G	G				G	G	G	Model
252	0.45	277				6930	0.007	1904000	Structure 2—sill din
N 90° E	N 90° E	N 71° E N 19° W				N 90° E	0	N 41° W N 49° E	re 2————direction
650 176	112 44	560 213				1500 180	450	3530 1271	range
	G								Model
	0.35								Str sill
	N 90° E								Structure 3
	600 342								range

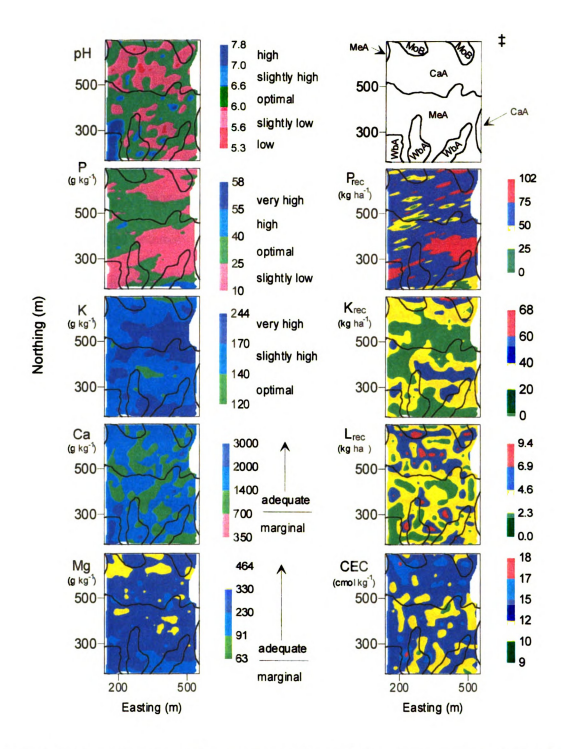


Figure 1.6. Contour maps of kriged soil variables and fertilizer recommendations using the FULL data sets overlain by the soil type boundaries †.

- \dagger CaA = capac loam with 0 to 4% slope; MeA = Metamora-Capac sandy loam with 0 to 4% slope; MeB = Morley Loam with 2 to 6 % slope; and WbA = Wasepi sandy loam with 2 to 6 % slope.
- ‡ indicates the soil types symbol designations

The RSVs for the first structure were greater than 50% with exceptions of K, ln(K) and K_{rec} so most of the variables could be described as being spatially structured (Figure 1.5; Table 1.4). The directional semivariogram models had ranges of spatial correlation of 34-m or greater in one of the two directions and the omnidirectional semivariogram models had ranges of at least 43-m. The degree to which these parameters affect the accuracy of SSFM predictions is of great interest but unknown.

The interpolated maps show that considerable areas of the field were low or slightly low in pH and slightly low in P. However, the entire field had greater than optimal K levels and greater than adequate Ca and Mg levels (Figure 1.6). As evident in these maps, the variables did not relate well with soil type. The apparent discrepancy between the ranges in Table 1.3 and Figure 1.5 is due to the smoothing effect of kriging that occurs with a non zero nugget effect (Goovaerts, 1997; Figure 1.5). Only when the nugget effect is zero does kriging behave as an exact interpolator.

Soil pH, P, and K had significant variability, the variability was spatially structured, and was in the manageable range. The variables were either normal or could be transformed to normality with log or normal score transformation. For some variables, the transformations also removed anisotropic features including directional, intrinsic stationarity. Unfortunately, normal score back transformations were problematic because of the nested, stair stepping features of the fertilizer recommendations. Because L_{rec}, P_{rec}, and K_{rec}, cannot be back transformed and deviate severely from normality, their SSFM may be difficult. Based on the presence of spatial structure and the fact that the variability was within the manageable range, there is potential for SSFM in this field but to determine if variability is adequately known, interpolations must be evaluated.

Phase II: Accuracy of SSFM sampling and interpolation

Grid Sampling

Grid sample design had an effect on semivariograms for all parameters (Figure 1.7). Anisotropy was not modeled for the reasons listed in the Phase I analysis. The semivariograms for the FULL (average grid size of 26.0-m) and the G_{comb} (average grid size of 29.2-m) data sets were similar. Because of the similarity, the test of the G_{comb} set against the VAL set discussed later should be indicative of the performance of the FULL data set. As sampling density decreases, the semivariograms deviate from those of the FULL data set. The semivariogram for the G_{30} data set has a higher nugget variance and range but a similar sill. The semivariograms for the four G_{61} and the G_{100} data sets deviated greatly from the FULL data set and from each other.

For kriging, the RMSE of the residuals of the predicted grid versus measured (VAL data set) generally increased as sampling intensity decreased with $G_{comb} < G_{30} < G_{61} < G_{100}$ (Figure 1.8). A spatial sampling scheme with utility should improve prediction over the whole field sample approach. The A_{30} field sampling scheme had the lowest RMSE for K and K_{rec} , which may relate to the fact that soil test K levels were high (low K_{rec}) and both K and K_{rec} had low RSV (Figure 1.7) or high nugget effects. It should also be noted that K was the only variable with substantial bias. The kriged G_{100} data sets had similar RMSE values to the field average approach for the remaining variables. The fact that the A_{100} field average had higher RMSE values for some variables than the A_{30} , illustrates the importance of obtaining a good estimate of the field mean, particularly in variables that are poorly spatially structured like K and K_{rec} .

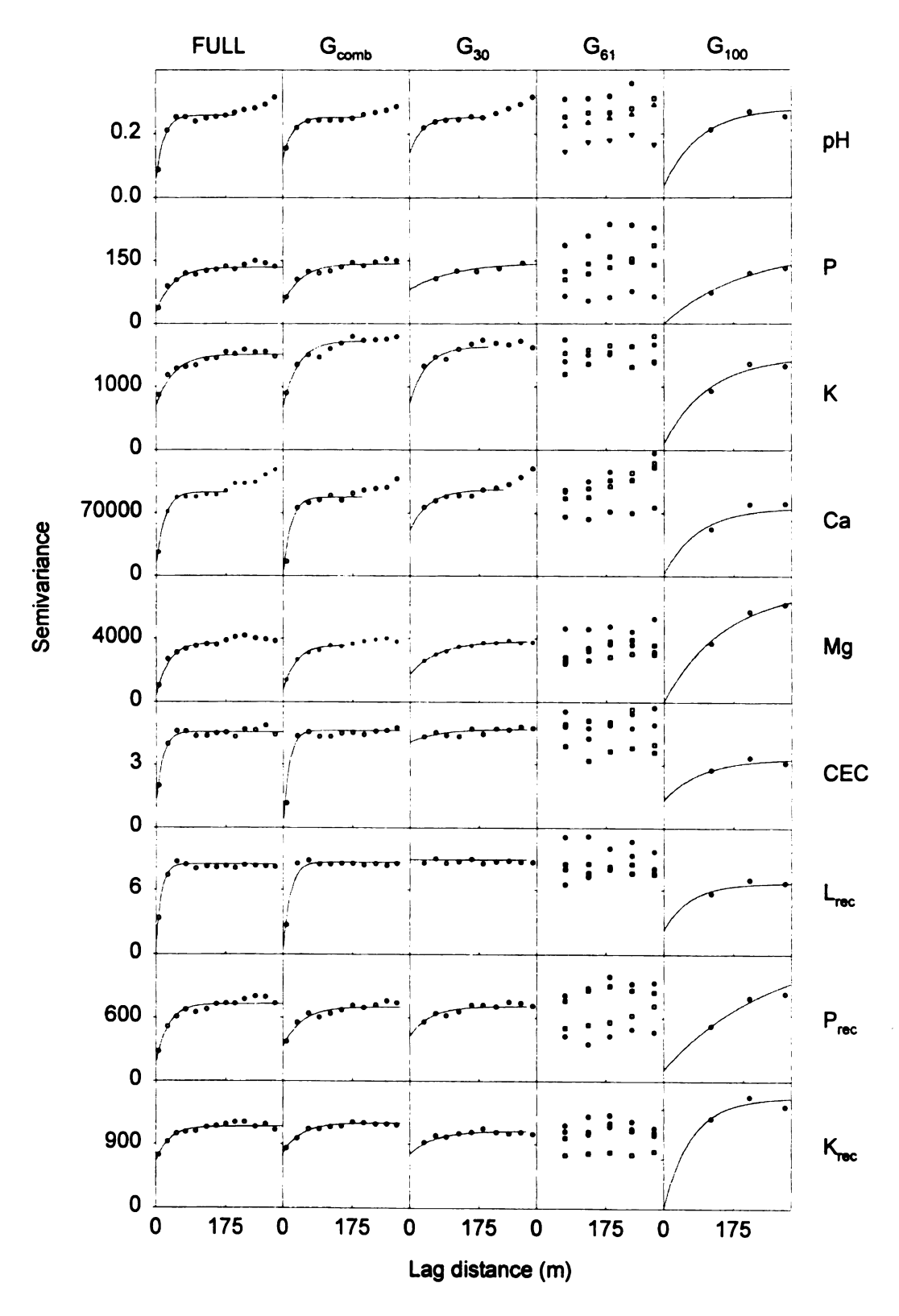


Figure 1.7. Omnidirectional experimental and modeled (exponential) semivariogram for the FULL, G_{comb} , G_{30} , G_{61} , and G_{100} data sets. [†]

† The semivariogram models for G₆₁ are not shown.

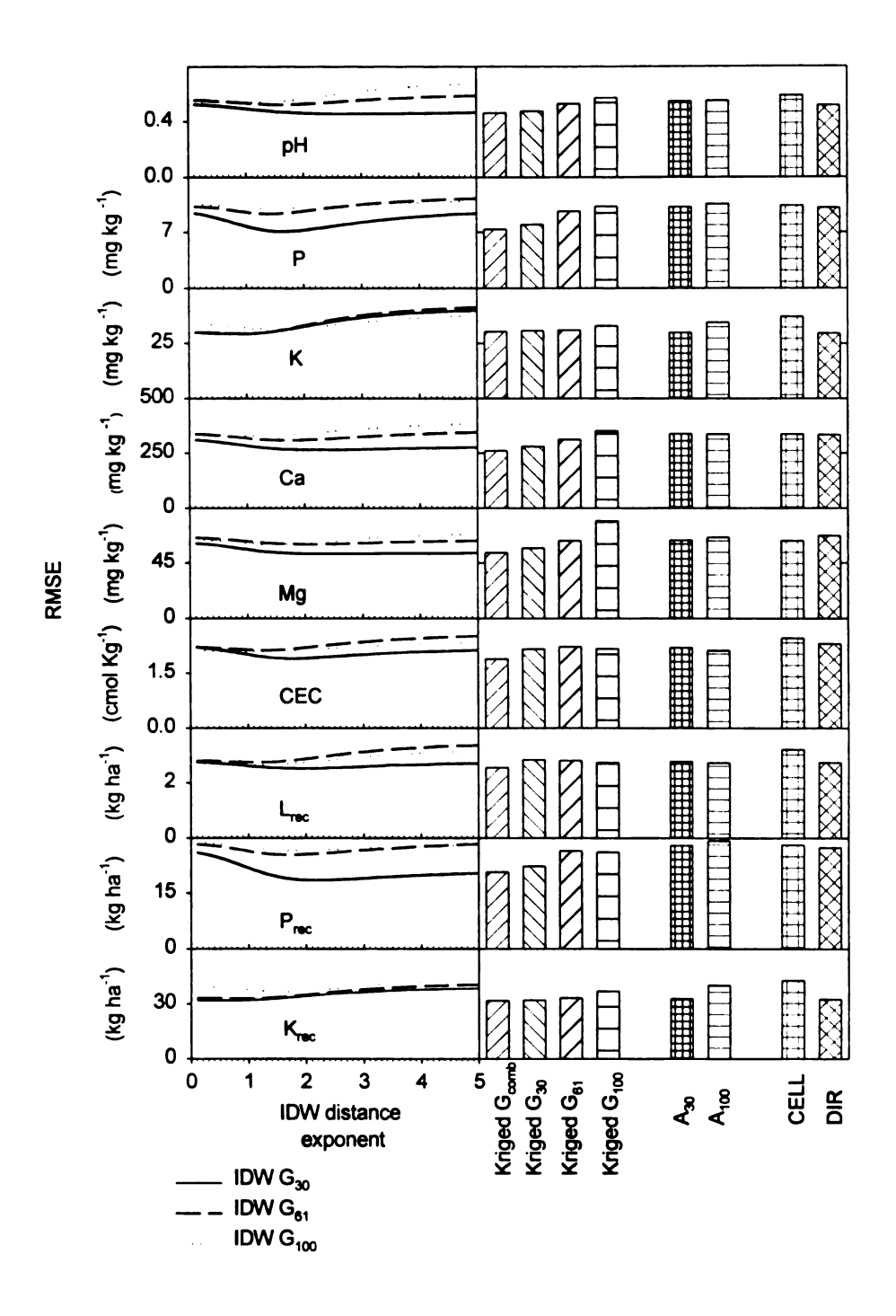


Figure 1.8. The RMSE for several estimation approaches: IDW interpolation for distance exponents ranging from 0.1 to 5.0 in 0.1 increments (line plots on the left), kriging, whole field, and grid cell sampling; and zone sampling.

Although kriging is often considered to be the most accurate interpolator, commercial SSFM applications commonly use IDW interpolation in lieu of kriging because it does not require modeling the semivariogram. Like kriging, the RMSE for IDW interpolation was affected by grid increment, but was also affected by the choice of the IDW distance exponent (Figure 1.8). Generally, RMSE decreased with increasing sampling intensity $G_{30} < G_{61} < G_{100}$ with the exceptions of CEC and L_{rec} . The RMSE decreased markedly for P and P_{rec} with an increase in sampling intensity from G_{61} to G_{30} while the RMSE for K and K_{rec} was reduced minimally. The RMSE decreased modestly for all variables with an increase in sampling intensity from G_{100} to G_{61} . The optimal distance exponent depended on the variable and sampling intensity. Consistent with the findings of Gotway et al. (1996), the value of each distance exponent was inversely related to the CV but only for the G_{30} and G_{61} data sets (Figure 1.9).

Measures of map error and prediction are indicators of map or prediction goodness but can not be completely understood without graphically comparing predicted and measured values along a 1:1 line (Figures 1.10). At the G_{100} sampling intensity, this relationship was generally weak for most variables. At the G_{30} sampling intensity, the relationship between predicted and measured values was moderate for P, and P_{rec} and marginal for the others. Even though, for G_{comb} , the relationship between predicted and measured markedly improved over this relationship for G_{30} , their regression lines were not parallel with the 1:1 line.

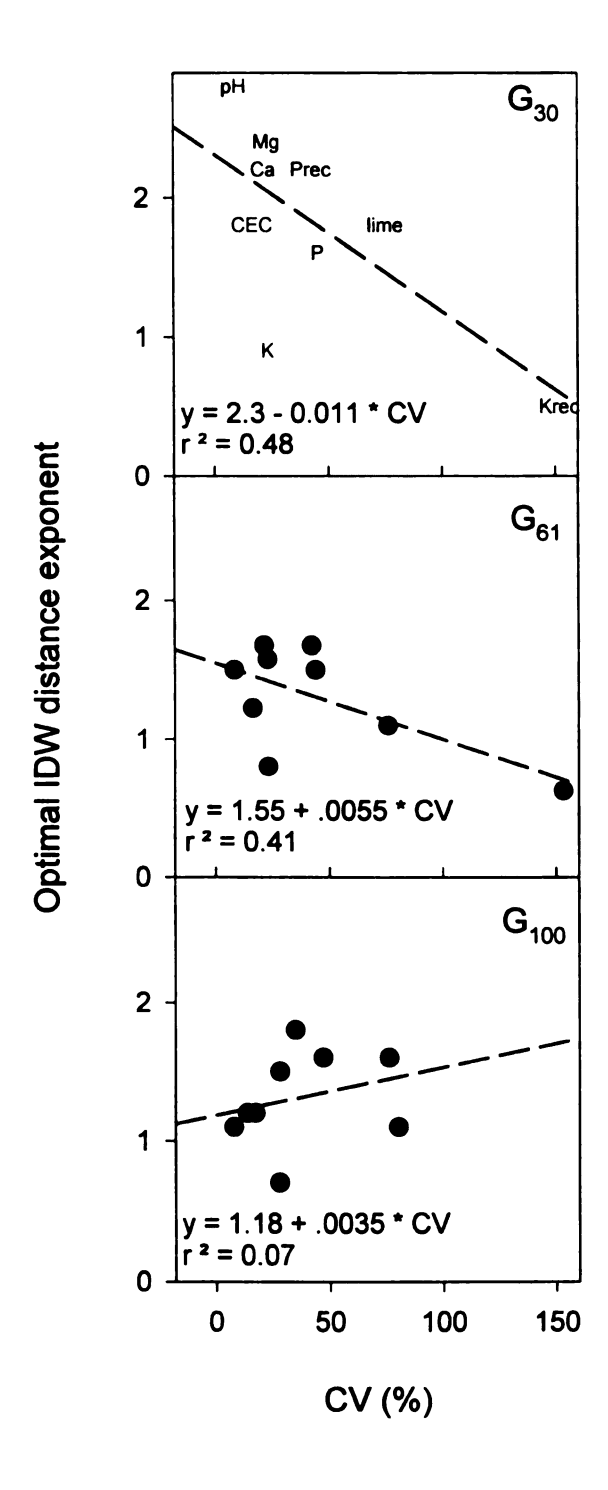


Figure 1.9. The relationship between the optimal distance exponent and the CV.

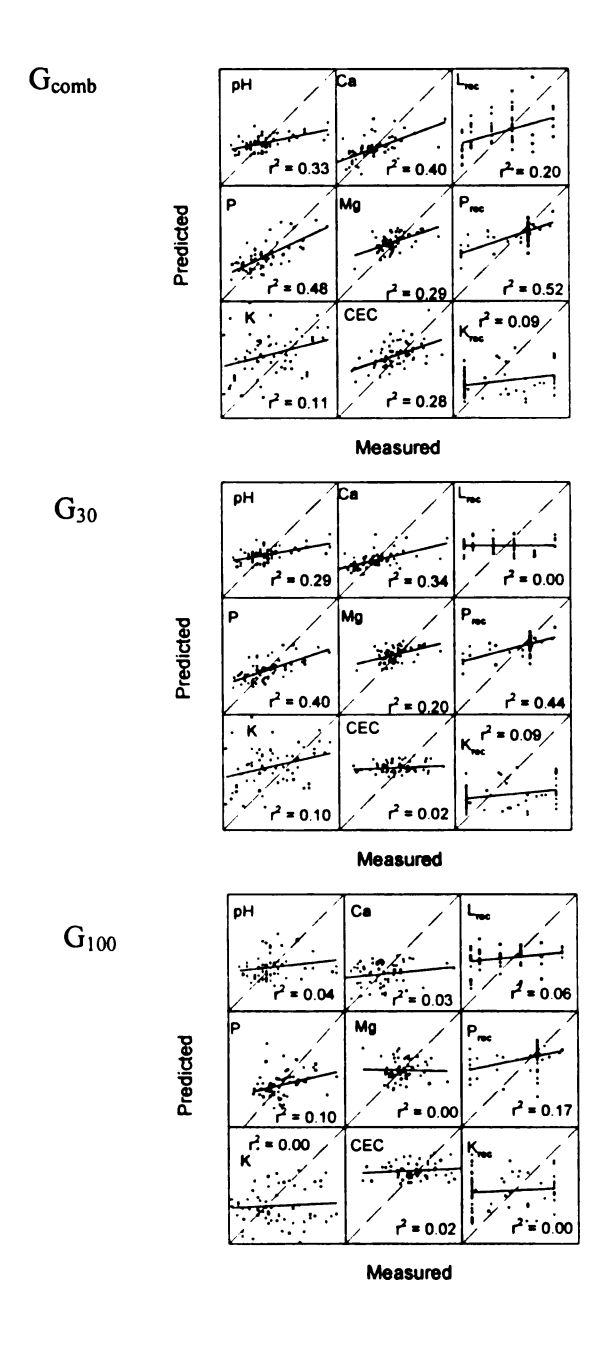


Figure 1.10. Predicted vs. measured for kriging with the G_{comb}, G₃₀, and G₁₀₀ data sets. †

† Dashed lines are the 1:1 lines. Solid lines are the regression lines.

Sadler et al. (1998) and Mohamed et al. (1996) suggest that the performance of SSFM at different grid intensities is a function of the spatial structure and range of spatial correlation of the spatial processes. The relationship between prediction efficiency, the range of spatial correlation, the RSV, and grid sampling increment are described in Figure 1.11. At each grid intensity, when the RSV values were less than 60 %, e.g. for K and K_{rec}, prediction efficiencies are low regardless of the fact that their ranges of spatial correlation were relatively high (greater than 90-m). For the G₃₀ data set, with the exception of Mg there was a quadratic relationship between prediction efficiency and the range of spatial correlation when RSV values exceeded 75% (Figure 1.12). While this relationship held for the G₆₁ data set, it does not exist for the G₁₀₀ data set. Therefore, inferences between geo-spatial studies and the expected performance of SSFM can be drawn but only when grid sampling intensities are adequate.

Using the optimal distance exponent, IDW was equal to or superior to kriging for most of the variables sampled on the 30, 61, and 100-m grid excluding log-transformed attributes (Figure 1.13). Unfortunately, there is no a priori knowledge of the optimal distance exponent. Visual inspection of Figures 1.13 suggests that a distance exponent of 1.5 would be a reasonable choice for this field. When the regression equations in Figure 1.12 were used to calculate the optimal distance exponent, the prediction efficiencies for the IDW approach were nearly the same as or slightly better than when the distance exponent was 1.5 with the exceptions of K and K_{rec} (Figure 1.13). How the relationship in Figure 1.12 holds for other soils or locations is not known. For both kriging and IDW interpolation, prediction efficiencies were lower for ln(P), and ln(Ca) than for P, and Ca. Although normalizing K improved the prediction efficiencies, they were

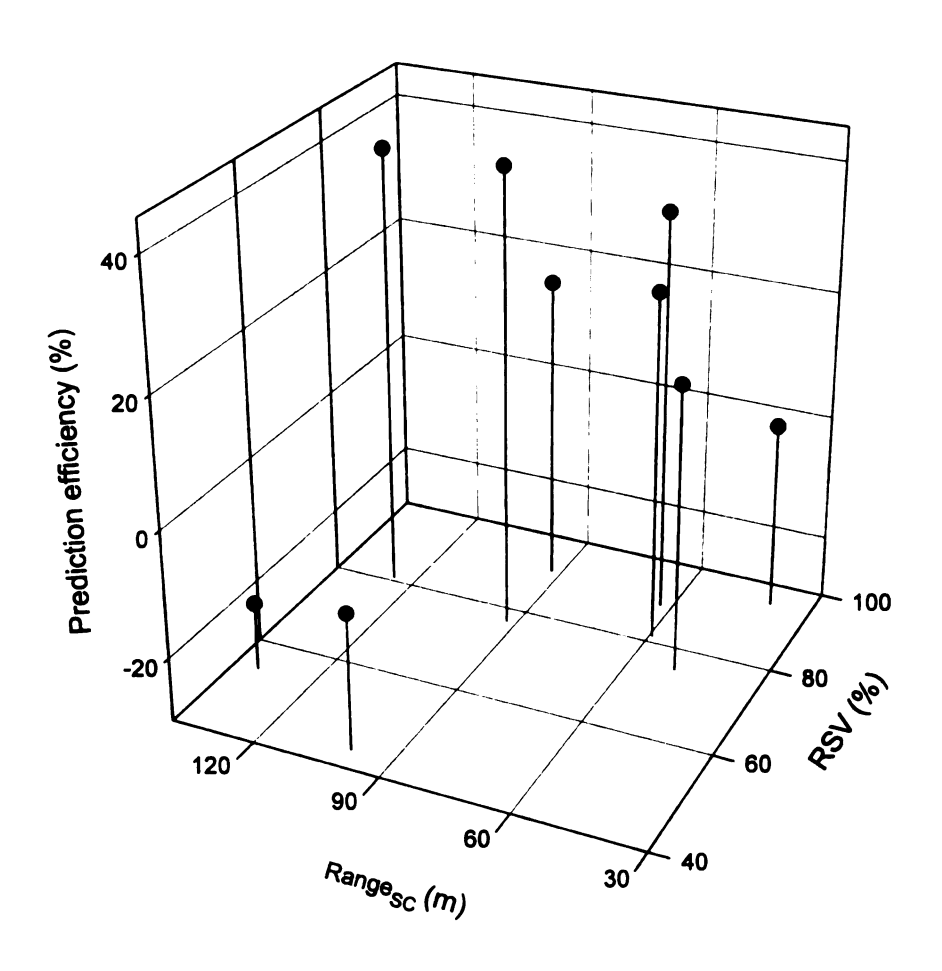


Figure 1.11. The relationship between prediction efficiency for kriging the G30 data set, the range of spatial correlation of the FULL data set, and the RSV of the FULL data set.

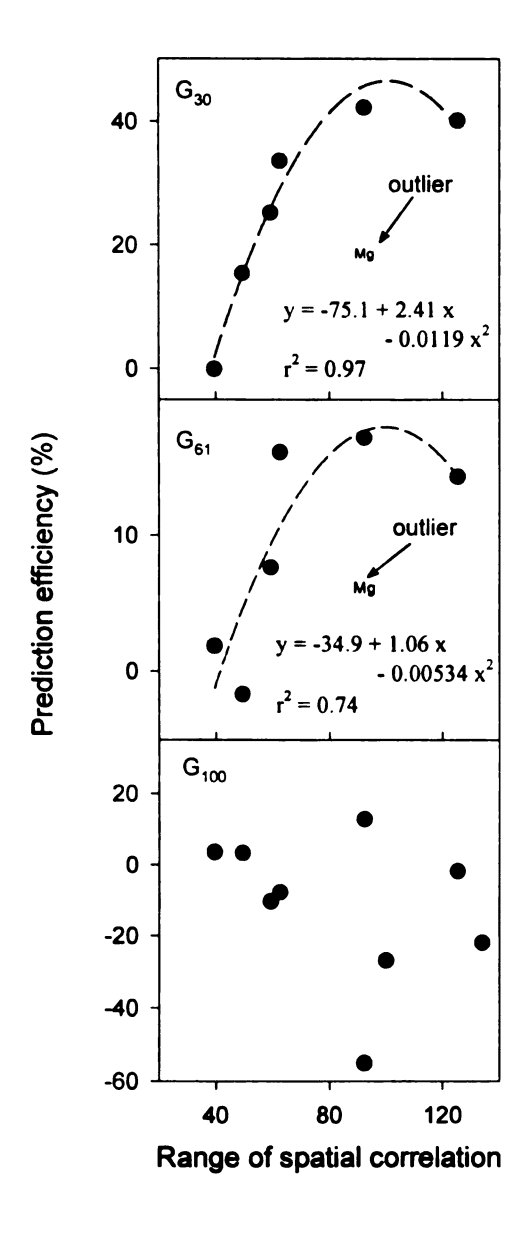


Figure 1.12. The relationship between prediction efficiency for the kriged G_{30} data set and the range of spatial correlation for the FULL data set for variables with RSV values greater than 70%.

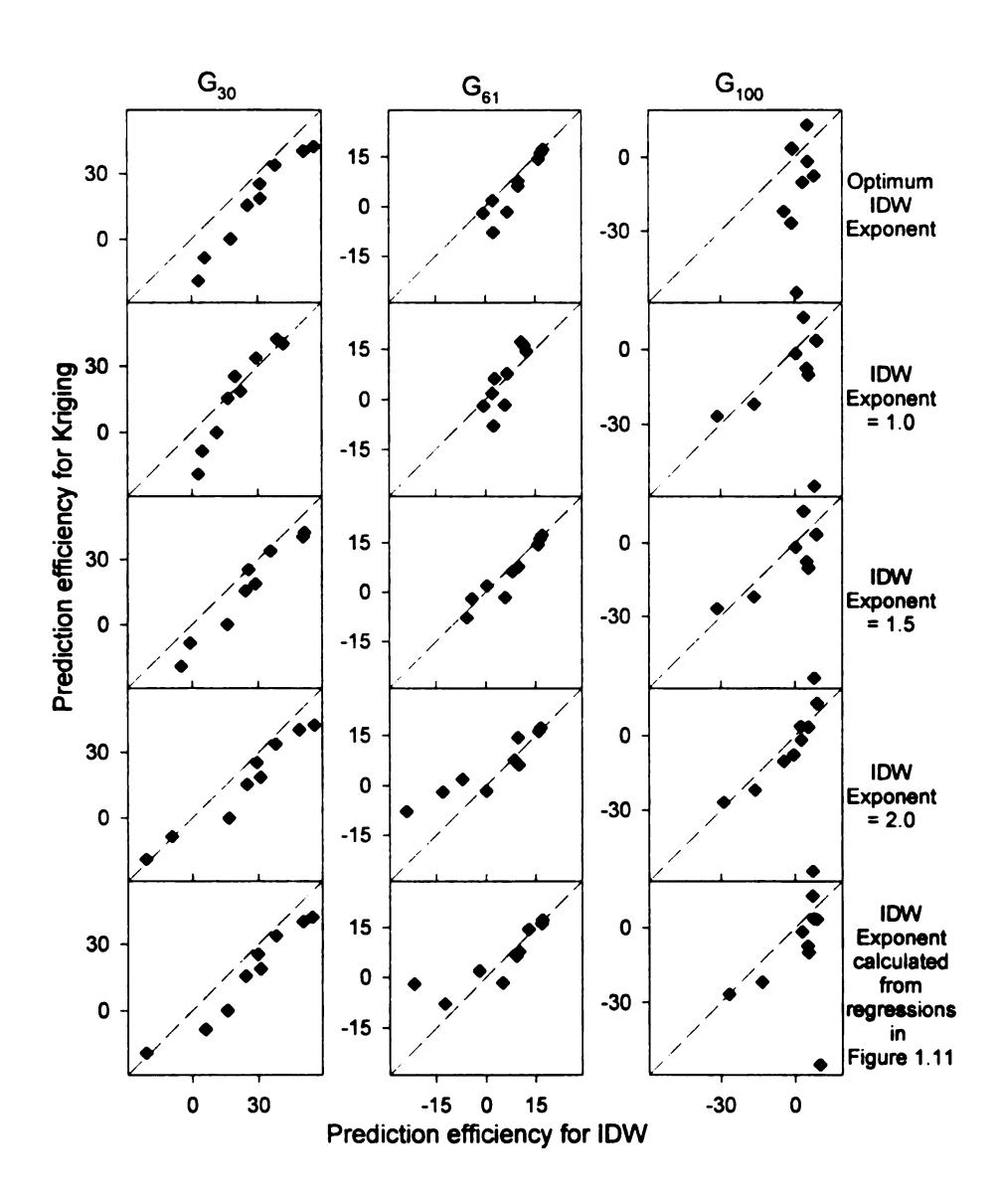


Figure 1.13. Prediction efficiency for kriging versus the prediction efficiency for IDW.

[†] Prediction efficiencies are for the G₃₀ data sets.

negative for K and ln(K), indicating that the field average approach was superior.

Normalizing the data had an insignificant or negative effect on the accuracy of the data.

The poor performance of kriging may be explained by the large variability of the semivariograms for individual pairs (Figure 1.14). A fitted semivariogram model to the average semivariograms would be accurate for a small fraction of the pairs. So for a kriged estimate, two sample points the same distance from the prediction point will be weighted the same even though the variances between the prediction points and the point to be estimated (if it were known) would vary widely. It may be that the scatter of the semivariogram cloud may be one of the best indicators of the spatial predictability of a given variable.

CELL and directed sampling

Alternatives to grid sampling include cell sampling and directed sampling. The CELL sampling approach had the highest RMSE for most variables (Figure 1.8) and the lowest prediction efficiencies, confirming the results of Wollenhaupt et al. (1994). The directed sampling approach had RMSEs that were similar to the A₃₀ field approach (prediction efficiencies near 0), indicating no advantage of directed sampling over the use of a mean value for this field (Figure 1.8).

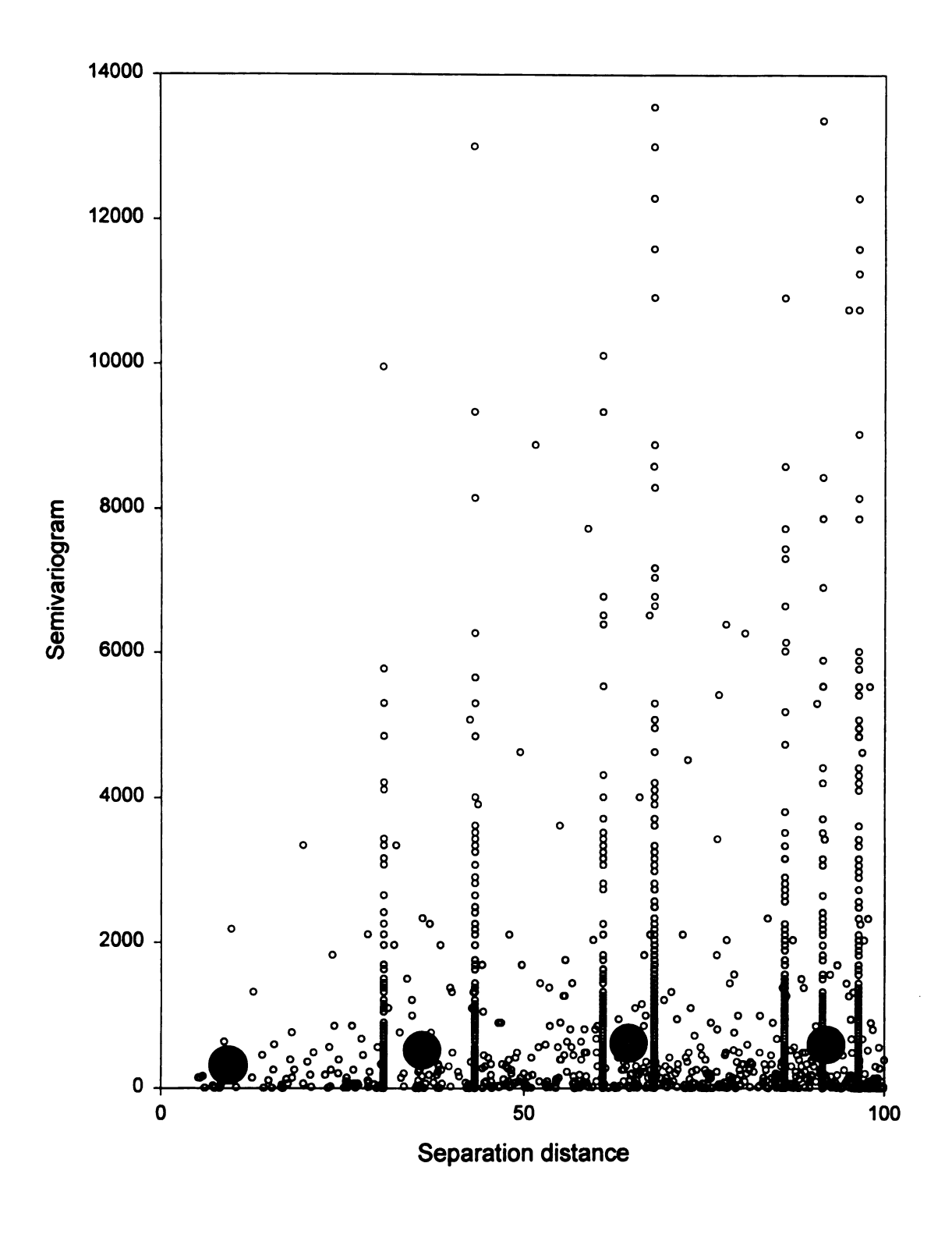


Figure 1.14. Average semivariograms (large solid circles) and semivariograms for individual pairs (hallow circles) for P using the G_{comb} data set.

CONCLUSIONS

Analysis of the FULL data set indicated that most soil fertility variables were spatially structured. Nevertheless, the presence of spatial structure alone did not prove sufficient for producing accurate yield maps, as evidenced by the plots of measured vs. predicted in Figures 1.10. Sampling at lower intensities increasingly diminished the delectability of spatial structure and generally increased the error of prediction as measured by RMSE. Where spatial structure was poor, particularly for K and K_{rec}, accurately sampling the field average was sufficient for nutrient management because SSFM for these variables was not appropriate. These data suggest that grid sampling at coarse grids and directed sampling were not adequate to produce accurate nutrient condition maps for this field. Cell sampling at least at the course 100-m grid intensity was also inadequate.

These data suggest that grid point sampling at the industry standard 100-m intensity was inadequate. Sampling at greater intensities only modestly improved prediction accuracy, likely not enough to justify the geometric increase in sampling costs. In the second chapter of this dissertation, I will examine methodology for incorporating secondary landscape information into spatial estimates of a soil property at several scales.

In this study, the accuracy of IDW interpolation with a distance exponent of 1.5 generally equaled or exceeded the accuracy of kriging at each scale of measurement. If the data had been strongly anisotropic or was not second order stationary, kriging may have been superior to IDW interpolation because the semivariogram model could account

for these peculiarities. The poor performance of kriging may be explained by the large variability of the semivariograms for individual pairs (Figure 1.14). Some measure of the scatter of the semivariogram cloud may be an indicator of the predictability in space.

CHAPTER 2

COMPARISON OF TECHNIQUES TO OPTIMIZE SPATIAL ESTIMATES OF SOIL PROPERTIES USING TERRAIN ATTRIBUTES

INTRODUCTION

Traditional survey methods and the more recent use of grid sampling and interpolation methods have not produced maps of soil properties with the accuracy needed for soil surveys (Bell et al., 1995; Moore et al., 1993) and precision farming (Pierce and Nowak, 1999; Robert, 1993). New analytical approaches are being used to utilize geometric properties of a landscape (slope, aspect, and curvature), collectively referred to as terrain attributes, to improve spatial estimates of soil properties. Terrain attributes are predictive of soil properties because topography is a soil forming factor. A high resolution, digital elevation model (DEM) is needed to calculate terrain attributes. Only recently has the technology become generally available to map elevation at the needed resolution, achieved through advances in high resolution global positioning system (GPS) now universally available. Several methods exist to use terrain attributes in spatial estimates of soil properties, ranging in complexity from simple regression to geostatistical methods. However, there is little consensus regarding which terrain attributes are most useful or which analytical method is most appropriate for a given soil property (Table 2.1).

Table 2.1. Applications of regression, kriging with an external drift, and cokriging for enhancing spatial estimates of soil properties using auxiliary information.

	Primary	Secondary	Measure of accuracy and or goodness †	Reported results †
		Regression		
Moore et al., 1993	A horizon depth $(R^2 = 0.51)$ soil P ($R^2 = 0.48$) soil pH ($R^2 = 0.41$) particle size ($R^2 = 0.64$)	4 terrain attributes	Visual comparison and the regression R ² values	
	43 points ha ⁻¹	43 points ha ⁻¹		variability
Bell et al., 1995	A horizon depth $(R^2=0.51)$ depth to free carbonates $(R^2=0.44)$	3 terrain attributes	VDS; plots of predicted versus measured	A- horizon and depths to carbonate predicted within 20 cm for 70% of validation samples
	7.25 points ha ⁻¹	75 points ha ⁻¹		validation samples
Thomson and Robert, 1995	Total carbon $(R^2 = 0.66 \text{ to } 0.69)$	2 terrain attributes and photographic tone	None	Unclear
	2.7 points ha ⁻¹	30 points ha ⁻¹		
Gessler et al., 1995	A horizon depth Solum depth	2 terrain attributes	Prediction error (not specific)	Regression reduced deviance by 63 and 68%
	scale not given Krig	scale not given ging with an external d	lrift (KED)	
Bourennane et al., 1996	Thickness of silty-clay- loam pedological horizon	. •	VDS; ME and RMSE	improvement over OK and KT
	0.62 samples ha ⁻¹	4.8 samples ha ⁻¹		
Gotway and	residual soil NO ₃ -1	corn grain yield		COK increased the
Harford, 1996	11 samples ha ⁻¹	66 samples ha ⁻¹	compared MSE for OK and KT with the MSE for KED	MSE by 7% over OK
Goovaerts, 1997	Soil Cd, Cu, Pb, and Co	Zn blocked estimates???	VDS; rank correlations for predicted and	Correlations between predicted and measured for
	(259 samples per field area)	(359 samples per field area)	measured and % misclassification	COK explain 16 to 35% more of the variability than for OK

Table 2.1, continued.

	Primary	Secondary Coloring (COV)	Measure of accuracy and or goodness	Reported Results	
Zhang et al., 1992 (COK with pseudo- crossvariogram)	NO ₃ -1 and Ca	Cokriging (COK) electrical conductivity	Cross validation, compared MSE for OK with MSE	cokriging reduced the MSE by 78%	
Vaughan et al., 1995	0.8 samples ha ⁻¹ Water content and soil salinity	1.3 samples ha ⁻¹ surface electrical conductivity	for COK Visual inspection	improvement over ordinary kriging	
	0.12 points ha ⁻¹	0.15 samples ha ⁻¹			
Rosenbaum and Söderström, 1996	Soil Cd	Soil Zn	Independent validation data set;	Correlation between predicted	
(standardized ordinary cokriging)	0.00034 points ha ⁻¹	0.0010 samples ha ⁻¹	correlation of predicted and measured	and measured wa greater for COK ($\rho = 0.85$) than OK ($\rho = 0.68$)	
Gotway and Harford, 1996	residual soil NO3	corn grain yield	Cross validation, compared MSE	COK reduced the MSE by 2%	
Harloid, 1990	10.8 samples ha ⁻¹	66 samples ha ⁻¹	for ordinary kriging with MSE for cokriging	WISE by 276	
Zhang et al., 1997	soil solute concentrations	soil solute concentrations measured at shallower depth	Cross validation, compared MSE for OK with MSE for COK	COK reduced the MSE between 30 and 60 %	
	1.3 - 1.8 points ha ⁻¹	1.3 - 1.8 samples ha ⁻¹			
Goovaerts, 1997 (isotropic and anisotropic standardized ordinary cokriging)	Soil Cd, Cu, Pb, and Co (259 samples per field area) ???	Four combinations of Ni, Zn, Pb, and or Cu.	VDS; correlations between predicted and measured and ME for both OK and COK	greater and errors	
Juang and Lee, 1998	Soil Cd and Zn	Soil Cd and Zn at same or lower depth	•	the r ² values by 6	
	2 points ha ⁻¹	5.5 points ha ⁻¹	(scale = 2 points ha ⁻¹) with OK predictions (scale = 5.5 points ha ⁻¹)	to 60% over COK.	

[†] VDS = Validation data set; MSE = Mean squared error; RMSE = Root mean squared error; ME = mean absolute error; SK = Simple Kriging; OK = Ordinary kriging; KT = Kriging with a trend model; COK = cokriging.

The simplest approach has been the use of simple or multiple regression in which a soil property is regressed on a single or multiple terrain attributes and the regression equation used to predict the soil property at unsampled locations within the field where terrain attributes are mapped. Success has been measured by the magnitude of the regression coefficient of determination (R²), which ranged from 0.41 to 0.69 for the studies reported in Table 2.1. In some cases, the accuracy of regression prediction was evaluated using a validation data set (Bell et al., 1995), which is a more robust accuracy measure.

The regression approach relies solely upon the relationship between the soil property of interest and the selected terrain attributes. Geostatistical prediction approaches utilize a statistical model of the spatial variability either using distance alone (ordinary kriging) or in conjunction with other measured variables (e.g., co-kriging). For ordinary kriging, a search radius is defined for each point that is to be assigned an estimate. A mean attribute value is calculated from sample data points within this radius and subtracted from each sample data point value. A weighted average of the residuals is calculated. The weights are based on an empirical, statistical model of the relationship between the separation distance and sample variance (semivariogram model). The neighborhood mean is added to the weighted average of the residuals to calculate an ordinary kriging point estimate. Estimation may be improved by incorporating secondary information into kriged estimates by substituting the mean term with a smoothly changing, rescaled variable (e.g. terrain attribute) that is linearly related to the variable being predicted, a procedure known as kriging with an external drift (Goovaerts, 1997; Deutch and Journel, 1998). Multiple secondary variables can be incorporated in this

fashion with a procedure known as random field analysis. However, this procedure has traditionally been used to remove spatial correlation from an analysis of variance (Stroup et al, 1994). Standardized ordinary co-kriging does not use the mean to incorporate secondary information. Rather, the prediction is the sum of the weighted averages of the primary variable and each of the secondary variables.

The performance of the various kriging approaches is mixed (Table 2.1). Goovaerts (1997) reports that, while correlated, kriging with an external drift and cokriging performed better than simple or ordinary kriging. In addition, cokriging performed better than kriging with an external drift for three of the four variables and anisotropic cokriging performed better than isotropic cokriging. However, Gotway and Hartford (1996) found that cokriging and kriging were respectively worse or only slightly better than ordinary kriging. The fact that correlations between residual nitrate and yield were not significant ($\rho = -0.09$) may explain the poor performance of these techniques.

From the studies in Table 2.1, there appears to be no consistency in which soil properties were analyzed, which terrain attributes were selected for prediction, the resolution of sampling of either soil properties or elevation, the scale of analysis, or the measures of accuracy of prediction, if used at all. Furthermore, the analytical techniques used in the various studies varied in complexity and in the effort required for analysis (regression < kriging with external drift << random field analysis << cokriging.

Increased complexity is only warranted if it leads to significantly improved spatial prediction. The objective of this study was to evaluate how different analytical techniques using terrain attributes affect the spatial prediction of soil properties and whether relative performance of these techniques is affected by the scale of soil sampling.

Four analytical techniques were used to generate spatial predictions of soil carbon obtained on 30 and 100 m regular grids using elevation, slope, and curvature as predictors and regression, residuals, and prediction efficiency as measures of performance.

MATERIALS AND METHODS

Site description

This study was conducted in a 12.5 ha field (47° 47' 30" N, 83° 52' 30 W) located 6-km south of Durand, Michigan in the Shiawassee River watershed (Figure 2.1). The field had been in a corn (Zea mays L.)-soybean (Glycine max L. (Merr.)) rotation for more than 10-yr. The soil color differences in the aerial photograph (Figure 2.1a) were related primarily to differences in soil organic matter content and drainage but did not match well with the second soil order survey map unit boundaries (Figure 2.1b). Because moisture conditions were not optimal in other years when USDA-AFS aerial photographs were taken (e.g. 1979, 1983, and 1992), the striking visual differences were not captured as they were in this photo (Figure 2.1a). The soil scientists who created this survey relied on aerial photography taken prior to 1958, which may have been of a lower quality or taken with a full crop canopy. With better aerial photos, there may have been a better match between the color differences in Figure 2.1a and the soil survey map unit boundaries.



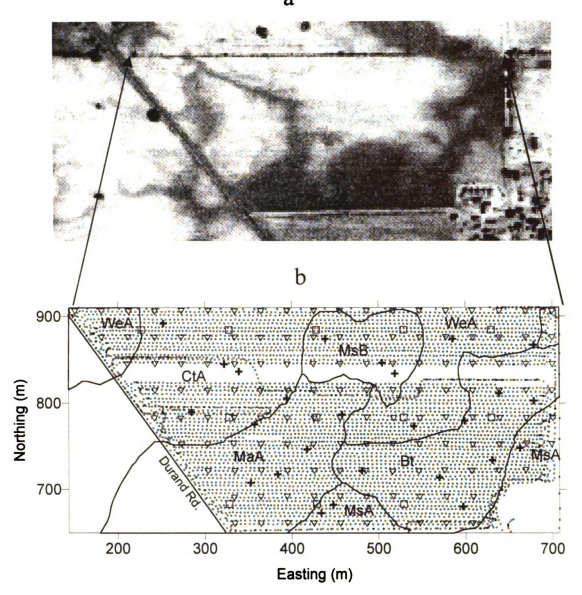


Figure 2.1. Study location: (a) areal photograph and (b) soil and kinematic GPS measurement locations overlain by soil type boundaries.

† The scanned and enlarged aerial photograph (original scale = 1:7,920; not georectified) taken 6/23/88 was purchased from the USDA-AFS Aerial Photography Field Office in Salt Lake City, UT. The locations of sample points for the three soil sampling strategies (G₃₀ = ∇; G₁₀₀ = □; VAL = +) and the kinematic survey (○) are overlain by NRCS soil map unit boundaries (Bt = Breckenridge sandy loam; CtA = Conover loam with 0 to 2 % slope; MaA = Macomb loam with 0 to 2 % slope; MsA = Metamora sandy loam with 0 to 2 % slopes; MsB = Metamora sandy loam with 2 to 6 % slopes; WeA = Wasepi sandy loam with 0 to 2 % slopes; Threlkeld and Feenstra, 1974).

Threlkeld and Feenstra (1974) classified and described the soils in Shiawassee County, MI at a scale of 1:20,000. The soils were mapped (Figure 2.1b) as somewhat poorly drained Alfisols with the exception of the Breckenridge (Bt; Coarse-loamy, mixed, nonacid, frigid Mollic Haplaquepts), a poorly drained Inceptisol. The Metamora sandy loam and Macomb loam (Fine-loamy, mixed, mesic Udollic Ochraqualfs) were very similar but the Metamora was coarser in texture which means that its surface drained somewhat faster but they both have slow subsurface drainage. While permeability is moderately rapid for the Wasepi (Coarse-loamy, mixed, mesic Aquollic Hapludalfs) series, it has low available water holding capacity. Most of the field had slopes of less than 2% except for the Metamora map unit with a B slope (MsB), ranging from 2 to 6%.

Soil Sampling Design and Laboratory Analysis

Soil samples were obtained from the field (Figure 2.1b) in May of 1997 using a 30.5-m (G_{30} ; n = 134; 10.7 samples ha^{-1}) regular grid, a 100-m (G_{100} ; n = 12; 1 sample ha^{-1}) regular grid, and a set of validation points (VAL; n=26; 2.1 samples ha^{-1}). The VAL points were collected using a 200 m unaligned grid with additional random points. The sample point locations were flagged using a DGPS system with a base station for on-thego differential correction. At the each sample locations, 5 sub-samples (1 at the grid point and 4 within a 1.5-m radius) were obtained to a depth of 20-cm using a 2.5-cm diameter soil core and composited. Soils were dried under forced air at 35° C for 3 days and pulverized to pass a 2-mm sieve. Sieved soil was finely ground with a roller mill and then analyzed for total carbon using a Carlo Erba NA 1500 Series 2 N/C/S analyzer (CE Instruments Milan, Italy). A 61-m grid (G_{61} ; n = 38; 2.7 samples ha^{-1}) was extracted from the G_{30} data set to be used as a third prediction data set.

DEM Creation and Terrain Analysis

A kinematic GPS survey was conducted in January of 1996 using two Z-12

Ashtech GPS sensors. The mobile GPS unit was mounted on an all terrain vehicle (ATV) traveling at about 17 km hr⁻¹ logging GPS location and elevation. Every second, a data point was logged so that the approximate distance between measurements was 4.7 meters. The ATV traversed the field in the east-west direction making swaths every 4.6 meters so the field was sampled at an approximate scale of 463 samples ha⁻¹. Data that had high position dilution of precision values (PDOP) and large vertical jumps between sequentially logged data points were removed. Several swaths were removed from the northern region of the field because of a systematic error in the GPS data (Figure 2.1b). Topogrid (ArcInfo ver. 7.1.1, ESRI 1997) was used to create a 1 × 1-m grid without drainage enforcement. Slope, aspect, and curvature (plan, profile, and tangential) were calculated with Surfer® (Golden Software, Golden, CO).

Data Analysis

For the G_{30} data set, normal probability (Q-Q) plots with 95 % confidence intervals (Friendly, 1991) were used to assess normality. Contour maps of semivariogram surfaces were created for total carbon and the terrain attributes to determine the direction of the anisotropic axes if anisotropy existed (Goovaerts, 1997; Isaaks and Srivastava, 1989). Directional (anisotropic) semivariograms were calculated for soil properties and terrain attributes using angular tolerances of \pm 22.5° for the soil variables (Goovaerts, 1997) and \pm 15° for terrain attributes (a smaller angle was used because terrain model was more densely sampled). For total carbon, nested semivariograms models

(combinations of spherical, exponential, and/or Gaussian models) if warranted, were chosen based on their fit to the empirical variograms. All variogram modeling was performed with Variowin (Pannatier, 1996). Correlations ($\alpha = 0.15$) and multiple regression ($\alpha = 0.15$) were calculated using SAS (SAS, 1990) for each grid sampling interval.

The G₃₀ and G₆₁ data sets were interpolated with regression, ordinary kriging, kriging with a trend model, kriging with an external drift, random field analysis, and standardized ordinary cokriging. Because there were so few points in the G₁₀₀ data set, only regression analysis was performed. All geostatistical interpolation methods were conducted with GSLib (Deutsch and Journel, 1998) except for random field analysis which was performed using SAS (SAS, 1990).

Some theoretical understanding is required to fully appreciate these procedures. A geostatistical prediction at an unobserved location s of an attribute Z is the weighted average of the observed values of the attribute at spatial locations s_i . The weights $w_{S(i)}$ may be restricted to non-zero values in some neighborhood $N_{(s)}$ of the target location s. If n(s) is the number of observed values in the neighborhood, the predicted value is calculated as

$$\hat{Z}_{K}(s) - m(u) = \sum_{i=1}^{n(s)} w_{s_{i}}[Z(s_{i}) - m(u_{i})]$$
 Eqn. 1

Goovaerts (1997, 1999) distinguishes between kriging interpolators by the treatment of the mean term m(u) or $m(u_i)$. The mean is constant throughout the study area for simple kriging (SK), and within each search neighborhood, but varies through the study area for OK, and varies gradually within each neighborhood $N_{(s)}$ for KT, KED,

and RFA. The mean component is modeled as a linear combination of the coordinates for KT, and as a linear function of a smoothly varying secondary variable (e.g. terrain attribute) for KED, and a linear or nonlinear combination of secondary variables for RFA. The kriging weights are calculated by solving the kriging system presented in Chapter 1 of this dissertation.

Measures of map error included MSE, RMSE (root mean squared error), and bias. Let v_i denote the differences between predicted value and observed value at location s_i , $i=1, ..., n_v = 62$ of the validation data set. Map errors and prediction efficiencies were calculated as described in the Introduction to the dissertation.

RESULTS AND DISCUSSION

The discussion here focuses on two issues. The first is whether variability in soil and terrain attributes within the field have the magnitude and structure needed for spatial prediction. Then interpolation methods that utilize terrain attributes will be evaluate using measures of prediction error and efficiency.

Nature of the Data

Due to its glacial origin, the elevation and derived terrain attributes within this field varied considerably (Figure 2.2). While total relief in the field is only 4 m, there is considerable micro-variability within the field as evidenced by rapid changes in slope and aspect over short distances. Therefore, micro-variability in terrain attributes may exert significant influence in the soil and hydrologic properties of this field. Elevation, slope and aspect (Figure 2.3) were normally distributed while plan curvature, profile curvature, and tangential curvature were not. Kriging or cokriging with non-Gaussian data is

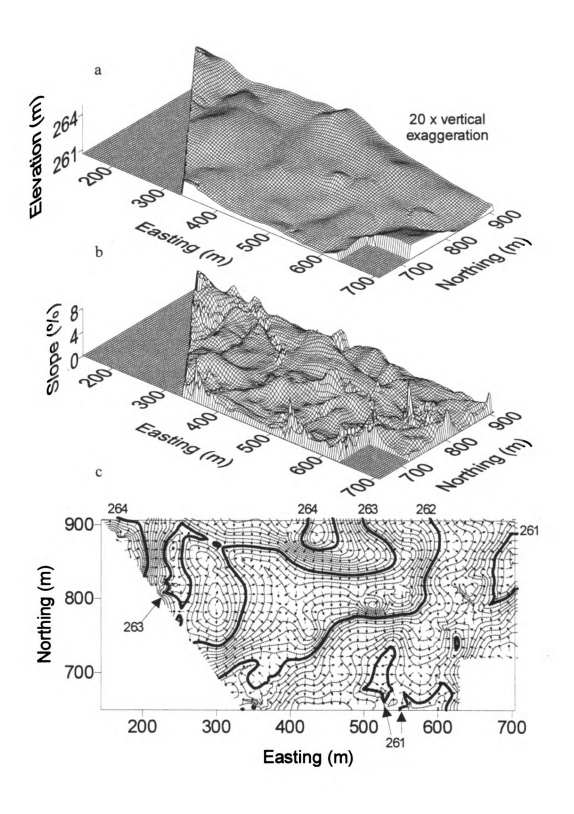


Figure 2.2. Surface maps (a) of elevation and (b) slope and a contour map (c) of elevation overlain with arrows indicating aspect.

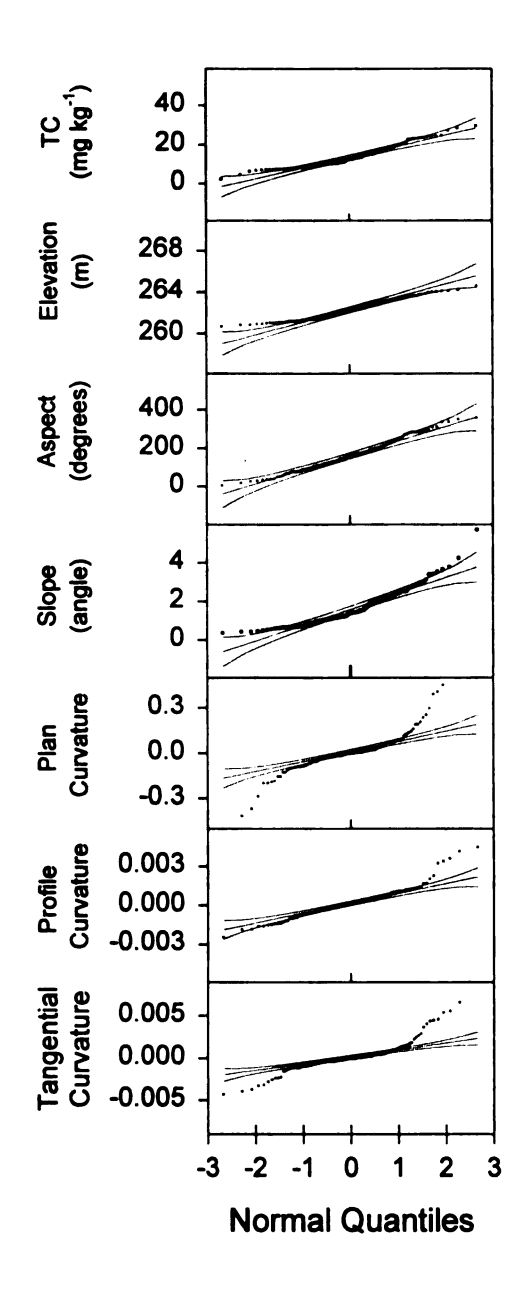


Figure 2.3. Normal probability (Q-Q) plots for variables and log transformation with 95% confidence intervals.

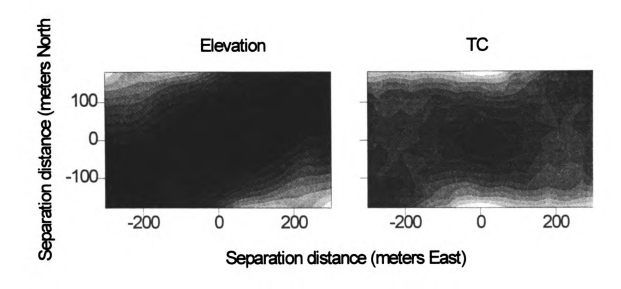


Figure 2.4. Semivariogram surfaces for total carbon (G_{30}) and elevation (n = 1000).

permissible but the predictions are not guaranteed to be best linear unbiased estimates (Cressie. 1993).

Elevation was severely anisotropic (Figure 2.4) with the axis of maximum spatial continuity 62° East from due North. Intrinsic stationarity was assumed in the orthogonal direction because the semivariogram did not reach a plateau. The anisotropic axes for slope were similar to the anisotropic axes for elevation except they were rotated 90° and were less severe (not shown). Plan curvature, profile curvature, and tangential curvature were mildly anisotropic (not shown).

The terrain attributes had large RSV values. Elevation had a range of spatial correlation of 275 m. Slope and aspect had ranges of about 70 m and the curvature parameters had ranges between 10 and 20 m. Elevation, slope and aspect were suitable to be used in a geostatistical analysis. The use of curvature in the geostatistical study is questionable because they were spatially correlated over such a short range and because they were not normally distributed.

Total carbon was normally distributed (Figure 1.3). The average value for the field was 13 g kg⁻¹, typical for a Michigan landscape. Despite just moderate changes in relief and slope (Figure 2.2), total carbon content ranged substantially (2 to 29 g kg⁻¹). The anisotropic axes occurred in the North-South and East-West directions but at distances of 200-m and greater the axes appear to shift to the same anisotropic axes system as for elevation (Figure 2.4). The RSV values were not as high as might be expected for total carbon which tends to be well structured (Table 2.2) indicating a large nugget effect. The nugget can not be accurately estimated when distances between sample points are great (e.g. 30.5 and 61-m). Therefore, the RSV could not be interpreted as a measure of spatial dependence for total carbon. The range parameters for the anisotropic model also was not interpreted because a technique had been employed to account for zonal anisotropic accomplished by manipulating the range parameters. The range of spatial correlation was quite large for the two isotropic models (244 and 249 m) indicating that the data were spatially well structured. Based on the large range of spatial correlation, total carbon is suitable for geostatistical analyses.

Ordinary kriging using the geostatistical parameters in Table 2.2 reveals that carbon values were generally lower in the on hill tops and in the northern region of the field and greater in the depressions in the southern and southeastern regions of the field (Figure 2.5). Unfortunately, however, much of the detail apparent in the aerial photo (Figure 2.1a) was not represented in this interpolation. In short, ordinary kriging did an adequate job of predicting soil carbon across the landscape but there is room for improvement. To apply other interpolation techniques, however, additional data requirements must be satisfied.

Table 2.2. Directional (G₃₀) and omnidirectional (G₃₀ and G₆₁) semivariogram model parameters for carbon to be used for ordinary kriging

	Structure 1						Structure 2			
	nugget	model	sill	direction	range (m)	RSV (%)	model	sill	direction	range (m)
Isotropic (G ₃₀)	6.2	s	31	0	249	75				
Anisotropic (G ₃₀)	10.2	G	15	N 90° E N 0° W	146 118	60	G	950	N 80° E N 10° W	20000 950
Isotropic (G ₆₁)	2.6	s	50	0	244	95				

[†] S = spherical; G = Gaussian; O = omnidirectional

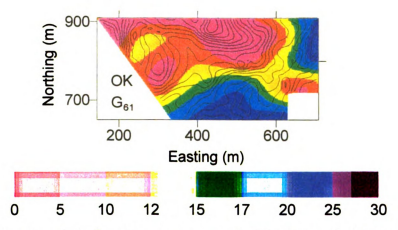


Figure 2.5. Total carbon (g kg⁻¹) contour map created with ordinary kriging using the G₃₀ data set overlain with elevation contours (lines).

For kriging with an external drift, the relationship between primary and secondary variables must be linear (Goovaerts, 1997). For cokriging variables must be both correlated and have structured cross semivariograms. Ahmed and De Marsily (1987) state that for cokriging to be of greater predictive value than ordinary kriging, the absolute value of the correlation coefficients between predicted and measured must

exceed 0.70 (Table 2.3). While most of the variables were significantly correlated with total carbon, only elevation could explain a substantial portion of its variability. In this study, elevation was the only variable suitable for cokriging and kriging with an external drift.

Table 2.3. Correlations between total carbon and terrain attributes and explained variability (G₃₀ data set) †.

	Correlations with Total Carbon	Variability in total carbon explained by terrain attributes (%)
Elevation	-0.72 *	51
Aspect	0.17	3
Slope	-0.40 *	16
Plan curvature	0.19 *	4
Profile curvature	0.20 *	4
Tangential curvature	0.21 *	4

[†] n = 134; * indicates significance at $\alpha = 0.05$

An important requirement for cokriging is that a linear model of coregionalization be developed that has covariance matrices that are positive semi-definite (Goovaerts, 1997). The parameters for the model at the G₃₀ scale are listed in Table 2.4. Another important requirement for kriging with a trend and kriging with an external drift is that a stationary trend exists. The models for the directional trend are presented in Table 2.5.

In summary, total carbon and elevation had sufficiently large correlations and structured semivariograms and cross semivariograms so ordinary kriging, and cokriging were appropriate methods. Because total carbon also had a directional trend, kriging with

Table 2.4. Linear model of coregionalization (G₃₀) used for cokriging..

			Structure 1 (Gaussian)		Structure 2 (Gaussian)			Structure 3 (Gaussian)		
SV [†] or Cross-SV	Nug [†]	Sill	Direction	Range (m)	Sill	Direction	Range (m)	Sill	Direction	range (m)
TC [†]		45	N 90° E	145	50	N 90° E	2000	6.2	N 62 E	6000
10	9	15	N 0° W	117	30	N 0°W	440	6.3	N 28 W	420
TC x	0.22	4 71	N 90° E	145	1 56	N 90° E	2000	2 61	N 62 E	6000
Elevation	-0.23	-1.71	N 0° W	117	-1.56	N 0° W	440	-3.61	N 28 W	420
			N 90° E	145	0.09	N 90° E	2000	- 4	N 62 E	6000
Elevation	0.02	0.225	N 0° W	117	3	N 0° W	440	2.1	N 28 W	420

[†] SV = semivariogram; Nug = nugget; TC = total carbon

Table 2.5. Semivariogram model parameters fo the direction of maximum spatial continuity (N 90 E) for kriging with a trend model and kriging with an external drift.

scale	nugget	model	sill	direction	range (m)
G ₃₀	9.4	G	16	N 90° E	190
G ₆₁	4.4	S	50	N 90° E	213

 $[\]dagger$ S = spherical; G = Gaussian

a (quadratic) trend and kriging with an external drift (elevation) were also appropriate methods. As will be presented in the next section, there were significant regression relationships between total carbon and the terrain attributes. Because of this, multiple regression and random field analysis are appropriate prediction methods.

Evaluation of Interpolation Methods

Stepwise regression ($\alpha = 0.15$) was used to predict total carbon each scale. The regressor variables were Easting (m), Northing (m), elevation (m), slope (%), plan curvature (m⁻¹), profile curvature (m⁻¹), and tangential curvature (m⁻¹) as independent variables; however, at each scale only various combinations of these regressors were selected to be in the model by the stepwise procedure.

Total Carbon (G_{30}) = 1451 - 5.45 × elevation - 0.0145 × Northing - 2.95 × slope + 3.24 × plan curvature + 619 × profile curvature

Total carbon (G_{61}) = 1567 - 5.88 × elevation - 0.0203 × Northing - 4.66 × slope + 18.6 × plan curvature - 993 × profile curvature

Total Carbon (G_{100}) = 59.48 - 0.0589 × Northing

More than half of the variability in total carbon was predicted at the G_{30} (R^2 = 0.66), G_{61} (R^2 = 0.77), and G_{100} (R^2 = 0.74) scales. At the G_{100} scale, only Northing was retained in the model and the R^2 for this relation was large. Visually, the gradient in TC is from N to S (Figure 2.1) and the few data points in the G_{100} grid could only identify this major trend. Therefore the regression from the G_{100} data set (n=12) represents spurious results because the measure of goodness were low. This is evident by a large RMSE, low prediction efficiency (Figure 2.6), and low r^2 between predicted and measured (Figure 2.7) for regression procedure at the G_{100} scale.

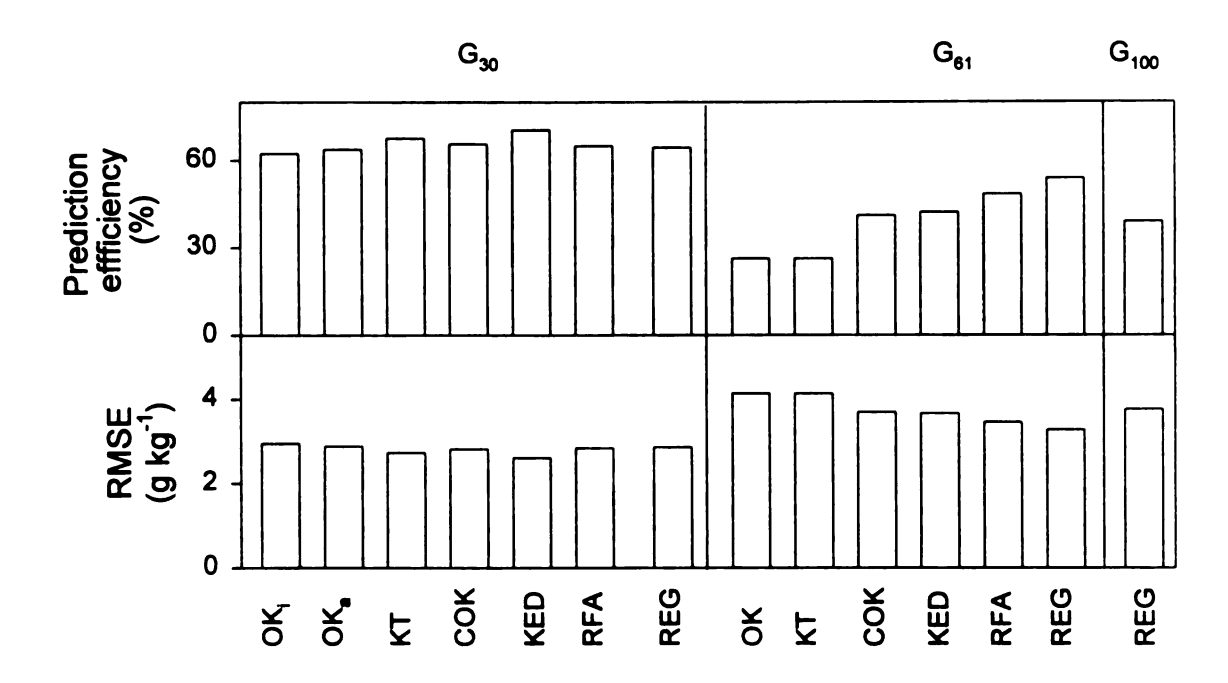


Figure 2.6. Prediction efficiencies and RMSE's.

† FA₃₀ = mean value of the G₃₀ data set; OK_i = isotropic ordinary kriging; OK_a = anisotropic ordinary kriging; KT = kriging with a trend; COK = cokriging; KED = kriging with an external drift; RFA = random field analysis.

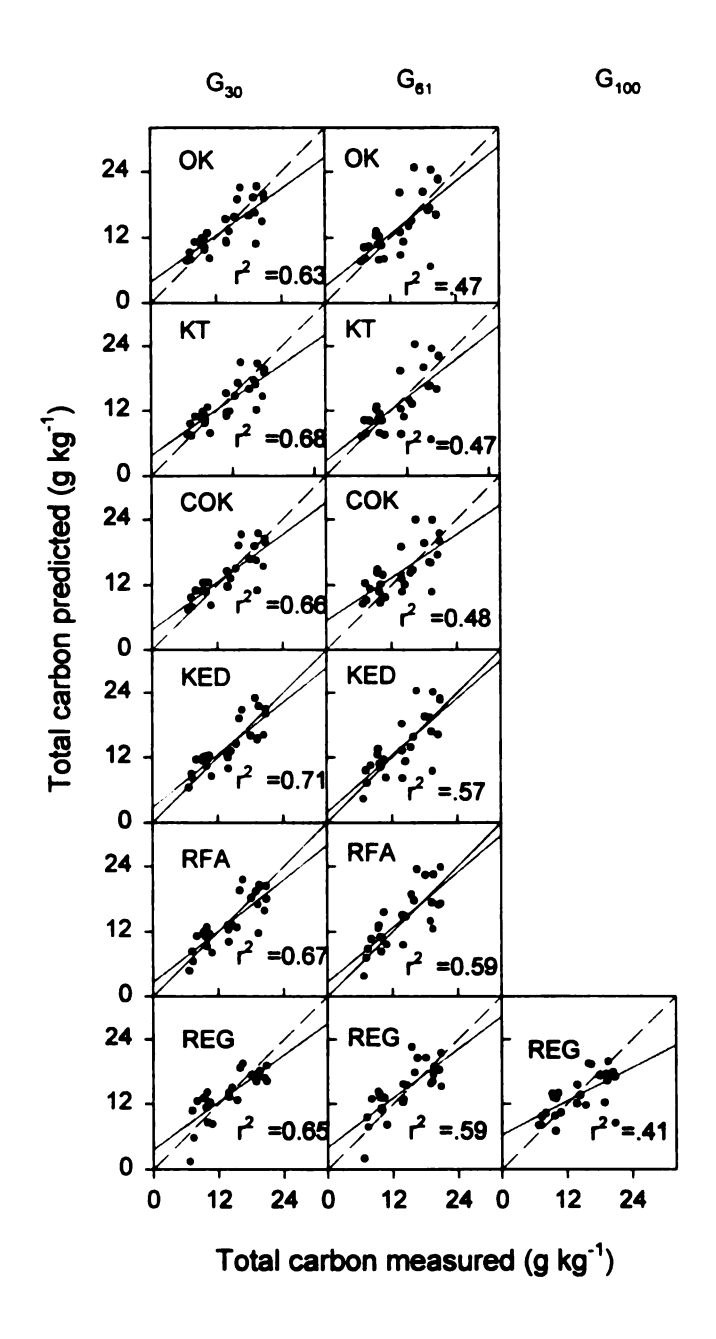


Figure 2.7. Predicted versus measured values for several prediction methods at two scales of measurement. †

† OK= isotropic ordinary kriging; KT = kriging with a trend model; COK = cokriging; KED = kriging with an external drift; RFA = random field analysis;

At the G₃₀ intensity, there was little difference between any of the prediction methods as assessed with measures of prediction efficiency and RMSE (Figure 2.6) or by deviations from a 1:1 line of predicted versus measured (Figure 2.7). At this scale, ordinary kriging and kriging with a trend model, methods which rely solely on a statistical model of the spatial variability, were of similar predictive value as methods that relied only on the relationship between total carbon and terrain attributes (multiple regression). Methods that utilized both the spatial variability of carbon and its relationship with other variables (e.g. kriging with an external drift) only performed slightly better than these methods.

At the G_{61} grid intensity, the regression approach had substantially lower RMSEs and higher prediction efficiencies than any other method at this scale. In fact, the RMSE for multiple regression was nearly in the same range as the RMSEs for the G_{30} interpolations (Figure 2.6). The plots of predicted versus measured show that at the 61-m grid scale, all of the methods that incorporated terrain information out performed those that used only geostatistical information, despite the large range of spatial correlation. A great deal of information about total carbon exists in the terrain attributes. The implication is that by using this information, it is possible to reduce the number of samples needed to achieve a certain level of accuracy.

The cost of soil sampling is inversely proportional to the square of the grid increment. For regression, prediction efficiency and grid sampling interval were inversely related (Figure 2.8) which allow the relationship between prediction efficiency and cost to be modeled. It should be noted that by considering the prediction efficiency, a squared loss function is assumed (since prediction efficiency is based on the MSE).

This is likely an incorrect assumption but unfortunately is the basis for most statistical measures of map error. In other words, an accurate understanding of the cost benefit relationship for grid sampling will require a better understanding of the relationship between map accuracy and the relative benefit to the farmer.

Recall that in Table 2.1, researchers who used the regression approach used the coefficients of determination (R^2) as an indicator of goodness. Figure 2.8 shows that the prediction efficiency decreases going from the G_{30} to G_{61} scales however the stepwise regression R^2 values increased from 0.66 and 0.77 for the G_{30} and G_{61} grids. This suggests that the R^2 may not be a very robust indicator of goodness.

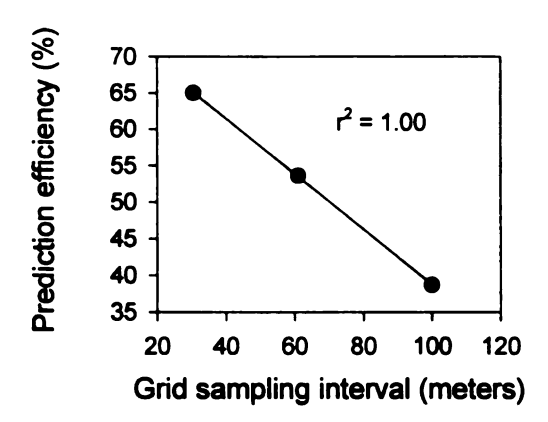


Figure 2.8. The relationship between prediction efficiency and sample point density for multiple regression interpolation.

Standard measures of prediction accuracy and efficiency are important. Some researchers use the correlations between predicted and measured while others compare MSE values (Table 2.1). Unfortunately, these measures are not the same and can give conflicting results. In Figure 2.7, the r^2 for ordinary kriging at G_{61} is 0.47 and the r^2 for

regression interpolation at G_{100} is 0.41 but the RMSE values are lower for ordinary kriging than for the regression interpolation (Figure 2.6). Clearly some standards are needed because these approaches can give conflicting results.

Although the predictions at the G_{30} intensity were not substantially different, kriging with an external drift performed the best based on higher correlation coefficients (Figure 2.7), greater prediction efficiencies, and lower RMSEs (Figure 2.6). However, the best interpolator at the G_{61} scale was multiple regression. The kriging with an external drift and multiple regression (G_{30} and G_{61}) interpolations have been overlain with elevation contours in Figure 2.9. Of these interpolations, by visual inspection, there is more correspondence between the kriging with an external drift interpolation and the aerial photograph (Figure 2.1a). In the southern and northeastern regions of the field, the kriging with an external drift interpolation matches the darker tones in the aerial photo better than the two multiple regression interpolations. But regression analysis does a better job of assigning high carbon values to low areas like the veiny feature in the west half of the field and low carbon values to ridges the bright red area in the north central region of the field. The regression approach is successful for these areas because the ridges and valleys have ether extremely positive or negative curvature values.

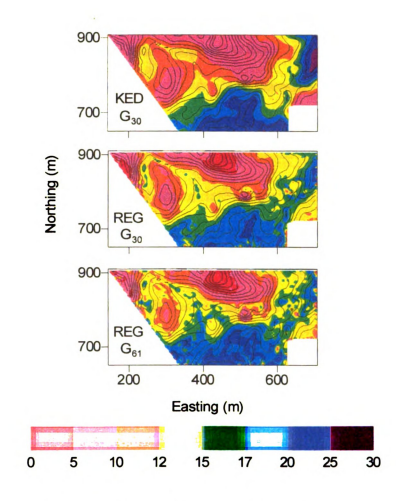


Figure 2.9. Predicted total carbon (g kg $^{-1}$) using kriging with an external drift (G₃₀) and multiple regression (G₃₀ and G₆₁).

[†] KED = Kriging with an external drift; REG = Multiple regression; For display purposes regressed interpolations were matrix smoothed (8 surrounding cells, central cell weight was 2.5; other 8 cells weights were 1)

CONCLUSIONS

Terrain attributes improved spatial predictions of total carbon particularly with the coarser sampling intensities. The comparable performance of multiple regression interpolation procedure suggests that it may not be necessary to use the more sophisticated geostatistical techniques. At high sampling densities (G_{30}) , interpolation method had little impact on overall map accuracy. There was an interaction between the scale of measurement and the most appropriate interpolation procedure. At lower sampling intensity (G_{61}) , methods that utilized terrain attributes were more precise than methods that did not. At this scale, multiple regression analysis yielded the best predictions, which were nearly as accurate as the methods sampled at the G_{30} scale.

By using techniques that incorporate terrain attributes, sampling intensity can be substantially reduced, while maintaining high levels of prediction accuracy and precision. Since the cost of grid sampling is inversely related to the square of the grid sampling increment, enhancing spatial estimates with terrain attributes is economically appealing.

SUMMARY AND RECOMENDATIONS

In the first chapter of this dissertation, grid sampling was found to be inadequate for accurate spatial predictions of soil chemical properties for a field in Clinton County, MI. The second chapter provides an example of how auxiliary terrain information (elevation, slope, aspect, and curvature) can successfully be used to enhance spatial estimates of total carbon. More work is needed to determine if terrain attributes can be used to enhance the predictions of soil fertility variables (e.g. pH, P, K). Additionally, other terrain attributes (e.g. wetness index, specific catchment area), high-resolution

multi-spectral images, electromagnetic conductivity, ground-penetrating radar could be used as secondary information.

Soil property sensors are greatly needed for precision agriculture, unfortunately there are few commercially available sensors that directly measure soil properties of agronomic importance. Development of on-the-go sensors for soil nutrients has been limited primarily to nitrogen and has not been very successful. Sensors for soil organic matter, water content, structure, compaction are still in development but have had greater success.

Until better sensors are developed, a two step approach is recommended. The first step is directed sampling based on field history, landscape features, remote sensed imagery, and yield map variability. Directed sampling may not provide accurate soil property maps. This was the case in the first chapter of this dissertation; however, management zones were based on NRCS soil types from a 1:15,840 survey. However, if a producer has records of within field manure applications or records of the locations of old field boundaries, this approach may prove to be quite accurate. The second step is the composite sampling of areas that have depressed yields or stressed plants as indicated in yield maps and remote sensed imagery. Plant nitrogen deficiencies can cause chlorosis, which changes the reflective properties of the plants. Chlorosis can be identified by aerial images.



BIBLIOGRAPHY

- Ahmed, S. and De Marsily, G. 1987. Comparison of geostatistical methods for estimating transmissivity using data on transmissivity and specific capacity. Water Resources Research, 23: 1717-1737.
- Bell, J.C., C.A. Butler, and J.A. Thomson. 1995. Soil-terrain modeling for site-specific agriculture management. p 208-227. In P.C. Robert et al. (ed.) Site -specific management for agriculture systems. ASA Misc. Publ. ASA, CSSA, and SSSA, Madison, WI.
- Bourennane, H. D. King, P. Chéry, and A. Bruand. 1996. Improving the kriging of soil variables using slope gradient as external drift. European journal of soil science. 47: 473-483.
- Brown, J.R. 1998.(ed.) Recommended Chemical Soil Test Procedures for the North Central Region. Missouri Ag Exp. Sta. Bul 1001.
- Cressie, N. 1993. Statistics for spatial data, revised edition. John Wiley & Sons, New York, 1991.
- Deutsch, C.V. and A.G. Journel. 1998. GSLIB: geostatistical software library and users guide, second edition. Oxford University Press, New York.
- Franzen, D.W. and T.R. Peck. 1995. Field soil sampling density for variable rate fertilization. J. Prod. Agric. 8(4): 568-574.
- Friendly, M. 1991, SAS system for statistical graphics, 1st edition, SAS Institute, Inc., Cary N.C.
- Gessler, P.E., I.D. Moore, N.J. McKenzie, and P.J. Ryan. 1995. Soil-landscape modelling and spatial prediction of soil attributes. Int. J. Geographical information systems. 9(4):421-432.
- Goovaerts. P. 1997. Geostatistics for natural resource evaluation. Oxford University Press, New-York. 483 pp.

- Goovaerts. P. 1999. Geostatistics in soil science: state-of-the-art prospective. In press. Geoderma.
- Gotway, C.A. R.B. Ferguson, G.W. Hergert, and T.A. Peterson. 1996. Comparison of kriging and inverse-distance methods for mapping soil parameters. Soil Sci. Soc. Am. J. 60:1237-1247.
- Gotway, C.A. and A.H. Hartford. 1996. Geostatistical methods for incorporating auxiliary information in the prediction of spatial variables. Journal of Agricultural, biological, and Environmental Statistics. 1(1): 17-39.
- Isaaks, E. and R. Srivastava. 1989. An introduction to applied geostatistics. Oxford University Press, New York, NY.
- Jaynes, D.B. 1996 Improved soil mapping using electromagnetic induction surveys. p. 169-179. *In.* P.C. Robert et al. (ed.) Proc. 3rd international conference on precision agriculture. ASA Misc. Publ., ASA, CSSA, and SSSA, Madison, WI.
- Juang, K.W. and D.Y. Lee. 1998. A comparison of three kriging methods using auxiliary variables in heavy-metal contaminated soils. J. Environ. Qual. 27:355-363.
- McCann, B.L., D.J. Pennock., C. van Kessel, F.L. Walley. 1996. The development of management units for site-specific farming. *In.* P.C. Robert et al. (ed.) Proc. 3rd international conference on precision agriculture. ASA Misc. Publ., ASA, CSSA, and SSSA, Madison, WI.
- Mohamed, S.B., E.J. Evans, R.S. Shiel. 1996. Mapping techniques and intensity of soil sampling for precision farming. p. 217 226. *In. P.C.* Robert et al. (ed.) Proc. 3rd international conference on precision agriculture. ASA Misc. Publ., ASA, CSSA, and SSSA, Madison, WI.
- Moore, I.D., P.E. Gessler, G.A. Nielsen, and G.A. Peterson. 1993. Soil attribute prediction using terrain analysis. Soil Sci.Soc. Am. J. 57:443-452.
- Pannatier, Y. 1996. Variowin: Software for spatial data analysis in 2D. Springer, New York, NY.
- Pierce, F.J. and Nowak. 1999. Aspects of precision farming. *In*. Advances in Agronomy. In Press.

- Pocknee, S. B.C. Boydell, H.M. Green, D.J. Waters, C.K. Kvien. 1996. Directed Soil Sampling. *In.* P.C. Robert et al. (ed.) Proc. 3rd international conference on precision agriculture. ASA Misc. Publ., ASA, CSSA, and SSSA, Madison, WI.
- Pregitzer, K.E. 1978. Soil survey of Clinton county, Michigan. Soil Conservation Service.
- Robertson, G.P., J.R. Crum, B.G. Ellis. 1993. The spatial variability of soil resources following long-term disturbances. Oecologia. 96:451-456.
- Robertson, G.P., K.M. Klingensmith, M.J. Klug, E.A. Paul, J.R. Crum, and B.G. Ellis. 1997. Soil Resources, microbial activity, and primary production across an agricultural ecosystems. Ecological Applications, 7(1): 158-170.
- Rosenbaum, M.S. and M. Söderström. 1996. Cokriging of heavy metals as an aid to biogeochemical mapping. Acta Agric. Scand. Sect. B, Soil and plant Sci. 46: 1-8.
- Sadler, E.J., W.J. Busscher, P.J. Bauer, and D.L. Karlen. 1998. Spatial scale requirements for precision farming: a case study in the southeastern USA. Agron. J. 90: 191-197.
- SAS Institute 1990. SAS/STAT user's guide. Version 6. SAS Inst., Cary, NC.
- Sayer, J.E. 1994. Concepts of variable rate technology with considerations for fertilizer application. J. Prod. Agric., 7(2): 195-201.
- Snyder, C., T. Schroeder, J. Havlin, and G. Kluitenberg. 1996. An economic analysis of variable rate nitrogen management. p. 989-998. *In P.C.* Robert et al. (ed.) Proc. 3rd international conference on precision agriculture. ASA Misc. Publ., ASA, CSSA, and SSSA, Madison, WI.
- Stroup, W.W., P.S. Baenziger, and D.K. Multize. 1994. Removing spatial variation from wheat yield trials: a comparison of methods. Crop Science. 34: p. 62-66.
- Sudduth, K.A., J.W. Hummel, S.J. Birrell. 1997. Sensors for site-specific management. p. 183-210. *In F.J. Pierce* and E.J. Sadler (ed.) The state of site-specific management for agriculture. ASA Misc. Publ., ASA, CSSA, and SSSA, Madison, WI.

- Thompson, W.H. and P.C. Robert. 1995. Evaluation of mapping strategies for variable rate applications p303-323. *In P.C.* Robert et al. ed.) Site –specific management for agriculture systems.. ASA Misc. Publ. ASA, CSSA, and SSSA, Madison, WI.
- Threlkeld, G.W. and J.E. Feenstra. 1974. Soil survey of Shiawassee county, Michigan. Soil Conservation service.
- Vaughan, P.J., S.M. Lesch, D.L. Corwin, and D.G. Cone. 1995. Water content effect on soil salinity prediction: a geostatistical study using cokriging. Soil Sci. Soc. Am. J. 59:1146-1156.
- Vitosh, M.L, J.W. Johnson, and D.B. Mengel: 1995. Tri-state fertilizer recommendations for corn, soybeans, wheat and alfalfa. Michigan State University Ext. Bull. E-2567.
- Wibawa, W.D., D.L. Dludlu, L.J. Swenson, D.G. Hopkins, and W.C. Dahnke. 1993. Variable fertilizer application based on yield goal, soil fertility, and soil map unit. J. Prod. Agric., 6(2): 255-262.
- Wollenhaupt, N.C., and D.D. Buchholz. 1993. Profitability of farming by soils. p. 199-211. *In* P.C. Roberts et al. (ed). Soil specific crop management. ASA Misc. Publ. ASA, CSSA, and SSSA, Madison, WI.
- Wollenhaupt, N.C., R.P. Wolkowski, and M.K. Clayton. 1994. Mapping Soil Test phosphorus and potassium for variable-rate fertilizer application. J. Prod. Agric. 7(4): 441-448.
- Zhang, R., D.E. Myers, and A.W. Warrick. 1992. Estimation of the spatial distribution of soil chemicals using pseudo-cross-variograms. Soil Sci. Soc. Am. J. 56:1444-1452.
- Zhang, R., P. Shouse, and S. Yates. 1997. Use of pseudo-crossvariograms and cokriging to improve estimates of soil solute concentrations. Soil Sci Soc. Am. J. 61:1342-1347.

MICHIGAN STATE UNIV. LIBRARIES
31293017665062